Turkish Journal of Earth Sciences (Turkish J. Earth Sci.), Vol. 21, 2012, pp. 905–932. Copyright ©TÜBİTAK
doi:10.3906/yer-1103-1 First published online 06 October 2011

Ion Probe U-Pb Dating of the Central Sakarya Basement: A peri-Gondwana Terrane Intruded by Late Lower Carboniferous Subduction/Collision-related Granitic Rocks

P. AYDA USTAÖMER[1], TİMUR USTAÖMER[2] & ALASTAIR. H.F. ROBERTSON[3]

[1] Yıldız Teknik Üniversitesi, Doğa Bilimleri Araştırma Merkezi, Davutbaşa-Esenler, TR–34210 İstanbul, Turkey (E-mail: ustaomer@yildiz.edu.tr)
[2] İstanbul Üniversitesi, Mühendislik Fakültesi, Jeoloji Bölümü, Avcılar, TR–34850 İstanbul, Turkey
[3] University of Edinburgh, School of GeoSciences, West Mains Road, EH9 3JW Edinburgh, UK

Received 01 March 2011; revised typescript receipt 24 August 2011; accepted 06 October 2011

Abstract: Ion probe dating is used to determine the relative ages of amphibolite-facies meta-clastic sedimentary rocks and crosscutting granitoid rocks within an important 'basement' outcrop in northwestern Turkey. U-Pb ages of 89 detrital zircon grains separated from sillimanite-garnet micaschist from the Central Sakarya basement terrane range from 551 Ma (Ediacaran) to 2738 Ma (Neoarchean). Eighty five percent of the ages are 90–110% concordant. Zircon populations cluster at ~550–750 Ma (28 grains), ~950–1050 Ma (27 grains) and ~2000 Ma (5 grains), with smaller groupings at ~800 Ma and ~1850 Ma. The first, prominent, population (late Neoproterozoic) reflects derivation from a source area related to a Cadomian-Avalonian magmatic arc, or the East African orogen. An alternative Baltica-related origin is unlikely because Baltica was magmatically inactive during much of this period. The early Neoproterozoic ages (0.9–1.0 Ga) deviate significantly from the known age spectra of Cadomian terranes and are instead consistent with derivation from northeast Africa. The detrital zircon age spectrum of the Sakarya basement is similar to that of Cambrian–Ordovician sandstones along the northern periphery of the Arabian-Nubian Shield (Elat sandstones). A sample of crosscutting pink alkali feldspar-rich granitoid yielded an age of 324.3±1.5 Ma, whilst a grey, well-foliated biotite granitoid was dated at 327.2±1.9 Ma. A granitoid body with biotite and amphibole yielded an age of 319.5±1.1 Ma. The granitoid magmatism could thus have persisted for ~8 Ma during late Early Carboniferous time, possibly related to subduction or collision of a Central Sakarya terrane with the Eurasian margin. The Central Sakarya terrane is likely to have rifted during the Early Palaeozoic; i.e. relatively early compared to other Eastern Mediterranean, inferred 'Minoan terranes' and then accreted to the Eurasian margin, probably during Late Palaeozoic time. The differences in detrital zircon populations suggest that the Central Sakarya terrane was not part of the source area of Lower Carboniferous clastic sediments of the now-adjacent İstanbul terrane, consistent with these two tectonic units being far apart during Late Palaeozoic–Early Mesozoic time.

Key Words: Central Sakarya basement, Ion Probe dating, zircon, Carboniferous, NE Africa

Orta Sakarya Temelinin İyon Prob U-Pb Yaşlandırması: Geç Erken Karbonifer Yaşlı Yitim/Çarpışma İle İlişkili Granitik Mağmatizma ile Kesilen Gondwana-Kenarı Kökenli Bir Blok

Özet: Kuzeybatı Anadolu'daki önemli bir 'temel' yüzeylemesinde yeralan amfibolit fasiyesi meta-kırıntılı sedimenter kayalar ile bunları kesen granitoidik kayaların göreli yaşlarını saptamak için iyon prob yaşlandırması yapılmıştır. Orta Sakarya temelindeki bir sillimanit-granat mika şistden ayrılan 89 kırıntılı zirkon mineralinin U-Pb iyon-prob yaş tayini 551 My (Ediyakaran)'dan 2738 My (Neoarkeen)'a kadar yaşlar vermiştir. Elde edilen yaşların yüzde seksenbeşi %90–110 konkordandır. Zirkon popülasyonları ~550–750 My (28 tane), ~950–1050 My (27 tane) ve ~2000 My (5 tane), daha küçük bir grup ise ~800 My ve ~1850 My'da kümelenmektedir. İlk, baskın popülasyon (geç Neoproterozoyik) Kadomiyen–Avalonya mağmatik yayı veya Doğu Afrika orojeni ile ilişkili bir kaynak alandan beslenmeyi yansıtır. Alternatif olarak Baltık kalkanı ile bir bağlantı çok zayıf bir olasılıktır. Çünkü Baltık kalkanı bu dönemin büyük bir bölümünde mağmatik açıdan pasif kalmıştır. Erken Neoproterozoyik yaşları (0.9–1.0 Gy), Kadomiyen bloklarındaki bilinen yaş aralığından önemli ölçüde sapma gösterir ve bunun yerine kuzeydoğu Afrika'nın bir bölümünden beslenme

ile uyumludur. Bu çalışmadan elde edilen Sakarya temelinin taşınmış zirkon yaş aralığı, Arap-Nubiya Kalkanının kuzey kenarı boyunca birikmiş Kambriyen–Ordovisyen kumtaşlarına (Elat kumtaşları) aşırı derecede benzerlik sergiler.

Orta Sakarya metamorfik temeli granitoyidik intrüzyonlar ile kesilir. Pembe, alkali feldspatca zengin bir granitoyid 324.3±1.5 My yaşı; gri, foliasyonlu biyotit granitoid 327.2±1.9 My yaşı vermiştir. Biyotit ve amfibol içeren bir diğer granitoyid kütlesinden ise 319.5±1.1 My yaşı elde edilmiştir. O nedenle, yitim veya Orta Sakarya blokunun Avrasya kenarına çarpışması ile ilişkili granitoyidik mağmatizmanın geç Erken Karbonifer döneminde ~8 My boyunca devam ettiği anlaşılmaktadır. Orta Sakarya bloku, Doğu Akdeniz bölgesindeki diğer 'Minoan' bloklarına göre daha önce, Erken Paleozoyik döneminde riftleşmiş ve daha sonra, olasılıkla Geç Paleozoyik döneminde Avrasya kenarına eklenmiş olmalıdır. Taşınmış zirkon topluluklarındaki farklılıklar, Orta Sakarya blokunun şu an bitişiğindeki İstanbul blokunun Alt Karbonifer kırıntılı sedimanları için bir kaynak alan oluşturmadığını, o nedenle bu iki tektonik birliğin Geç Paleozoyik–Erken Mesozoyik döneminde birbirlerinden oldukça uzak olduklarını göstermektedir.

Anahtar Sözcükler: Orta Sakarya temeli, İyon Prob yaşlandırması, zirkon, Karbonifer, KD Afrika

Introduction

U-Pb detrital zircon age populations in terrigenous sedimentary or metasedimentary rocks can be used to infer the source regions of exotic terranes in orogenic belts. This can be achieved by comparing the ages of tectono-thermal events recorded in the zircon grains with the source ages of the potential source cratons. U-Pb detrital zircon ages can also provide a maximum age of deposition for clastic sediments, which is particularly useful where the rocks are metamorphosed or unfossiliferous. The dates of cross-cutting igneous intrusions can be combined with the ages of detrital zircons to provide additional constraints on the timing of deposition. We use this approach here to shed light on the potential source region of the Central Sakarya basement (~Sakarya Continent) in N Turkey, where granitoid rocks cut previously undated schists and paragneisses.

Turkey is made up of a mosaic of continental blocks separated by dominantly Late Cretaceous–Cenozoic ophiolitic suture zones (Şengör & Yılmaz 1981; Okay & Tüysüz 1999; Figure 1). In particular, the İzmir-Ankara-Erzincan suture zone separates the Triassic rocks of the Pontides to the north (correlated with Eurasia) from the Anatolides and Taurides to the south (correlated with Gondwana). The Pontide tectonic belt of northern Turkey is itself a composite of several terranes. Two major continental blocks are exposed in the northwest Pontides, namely the Istranca Massif and the İstanbul terrane (Figures 1 & 2). The Istranca Massif comprises a Palaeozoic metamorphic basement, unconformably overlain by Triassic–Jurassic metasedimentary rocks (A.I. Okay *et al.* 2001a; Sunal *et al.* 2011). The adjacent İstanbul terrane exposes an unmetamorphosed, transgressive sedimentary succession of Ordovician to Early Carboniferous age, with an unconformable Triassic sedimentary cover (Abdüsselamoğlu 1977; Şengör 1984; Özgül 2012). The Palaeozoic succession of the İstanbul terrane begins with Ordovician red continental clastic rocks and shallow-marine sedimentary rocks. Platform sedimentation persisted until the Late Devonian when rapid drowning of the platform was associated with the deposition of pink nodular limestones coupled with intercalations of radiolarian chert (Şengör 1984; T. Ustaömer & Robertson 1997; P.A. Ustaömer *et al.* 2011; N. Okay *et al.* 2011; Özgül 2012). Sedimentation continued with deposition of black ribbon cherts containing phosphatic nodules and this was followed by a Lower Carboniferous turbiditic sequence (Şengör 1984; N. Okay *et al.* 2011; Özgül 2012).

The more easterly part of the Pontide tectonic belt includes the Sakarya Zone (Okay & Tüysüz 1999), also known as the Sakarya Composite Terrane (Göncüoğlu *et al.* 1997). The Sakarya Zone is characterised by a Lower Jurassic to Upper Cretaceous sedimentary succession that is interpreted to record the development of a south-facing passive margin (Şengör & Yılmaz 1981; Y. Yılmaz *et al.* 1997). The passive margin switched to become part of a regional Andean-type active margin during the Late Cretaceous (Y. Yılmaz *et al.* 1997). A regional Mid-Eocene unconformity above the Mesozoic succession is interpreted as the result of a collision of the Sakarya Zone with the Anatolide-Tauride Platform to the south (Y. Yılmaz *et al.* 1997; A.I. Okay & Whitney 2011).

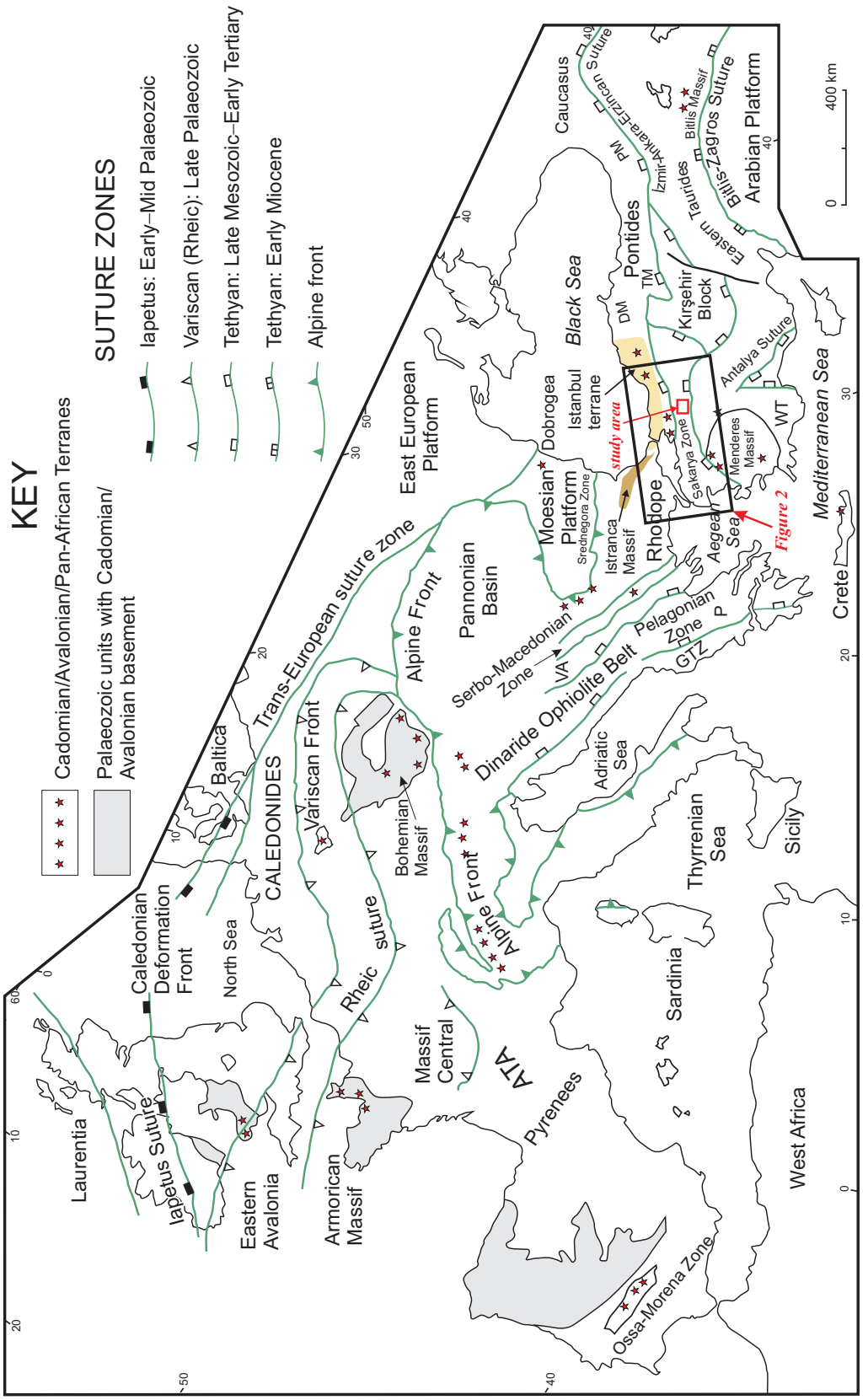

Figure 1. Tectonic map showing the locations of Cadomian-Avalonian basement units in Europe and the Eastern Mediterranean area. Suture zones of Turkey are indicated. Red box indicates the study area and the black box the location of Figure 2. Data sources: Quésada (1990), Abramovitz *et al.* (1999), Guterch *et al.* (1999), Miller *et al.* (1999), Unrug *et al.* (1999), Chantraine *et al.* (2001), Savov *et al.* (2001), Bandres *et al.* (2002), Chen *et al.* (2002), Dörr *et al.* (2002), Gubanov (2002), Linnemann & Romer (2002), Murphy *et al.* (2002), Pin *et al.* (2002), Romano *et al.* (2004), Gürsu & Göncüoğlu (2005), Okay *et al.* (2008b); P.A. Ustaömer *et al.* (2005, 2009). ATA– Armorican Terrane Assemblage, DM– Devrekani Metamorphics, GTZ– Gavrovo-Tripolitza-Ionian Zone, P– Pindos Zone, PM– Pulur Metamorphics, TM– Tokat Massif, VA– Vardar-Axios Zone, WT– Western Taurides. The base map uses the Lambert projection.

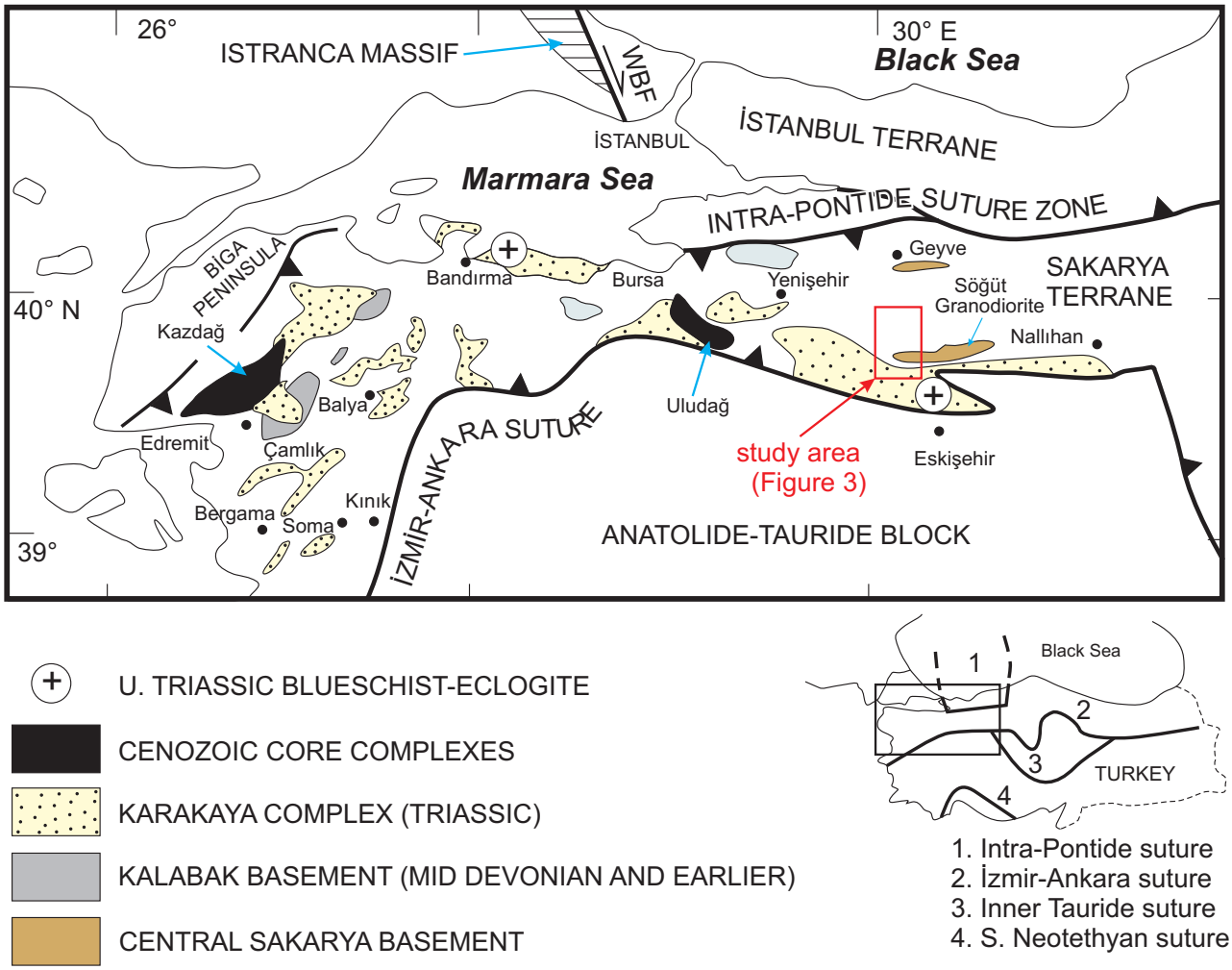

Figure 2. Tectonic map of NW Anatolia showing the various basement terranes of the Sakarya Zone and the Variscan continental units to the north (İstanbul terrane and the Istranca Massif). The contact between the İstanbul terrane and the Istranca Massif is inferred to be a right-lateral strike-slip fault zone (West Black Sea Fault: WBF), active during opening of the West Black Sea oceanic basin in the Late Cretaceous (A.I. Okay *et al.* 1994). The Intra-Pontide Suture Zone formed during the Late Cretaceous related to closure of Tethyan ocean to the south (Şengör & Yılmaz 1981; Robertson & Ustaömer 2004). The İzmir-Ankara Suture (İAS) which formed during Early Cenozoic is the most prominent suture zone in Turkey as it separates the Eurasian and Gondwanan terranes to the north and south (Şengör & Yılmaz 1981; Okay & Tüysüz 1999; Robertson *et al.* 2009). Inset: the main suture zones of Turkey. Modified after Okay 2010 and Robertson & Ustaömer 2012. Red box shows the location of the study area shown in Figure 3.

The pre-Lower Jurassic basement of the Sakarya Zone is dominated by the Karakaya Complex, which is widely interpreted as a Triassic subduction-accretion complex related to northward subduction beneath a continental margin arc terrane (Tekeli 1981; Pickett & Robertson 1996, 2004; A.I. Okay 2000; Robertson & Ustaömer 2012). Associated metamorphosed continental units (e.g., Central Sakarya basement; Pulur Massif) are correlated with this Palaeozoic active margin.

Metamorphosed continental units are exposed in several inliers along the length of the Pontides (Figure 1). From west to east these are the Kalabak basement (A.I. Okay *et al.* 1991; A.I. Okay & Göncüoğlu 2004; Pickett & Robertson 2004; Robertson & Ustaömer 2012; Aysal *et al.* 2011), the Central Sakarya

basement (Y. Yılmaz 1977, 1979; Y. Yılmaz *et al.* 1997; Göncüoğlu *et al.* 1996) and the Pulur Massif (Figures 1 & 2; Topuz *et al.* 2004; T. Ustaömer & Robertson 2010). Smaller continental units further east include the Devrekani metamorphics in the Central Pontides (O. Yılmaz 1979; Tüysüz 1990; T. Ustaömer & Robertson 1993, 1997; Nzegge *et al.* 2006) and the Tokat Massif in the Eastern Pontides (Figure 1; Y. Yılmaz *et al.* 1997). The basement units as a whole are typically exposed in the hanging walls of large thrust sheets (Y. Yılmaz 1977; A.I. Okay & Şahintürk 1997; T. Ustaömer & Robertson 2010), with a Jurassic sedimentary cover above. Two additional large metamorphic massifs, the Kazdağ Massif and the Uludağ Massif, are exposed beneath the Karakaya Complex in the western Pontides (Figure 2). The Uludağ (A.I. Okay *et al.* 2008c) and Kazdağ Massifs in particular still remain poorly dated (Erdoğan *et al.* 2009).

The Kalabak basement includes cross-cutting granites, which are radiometrically dated as Early to Mid-Devonian (A.I. Okay *et al.* 1996, 2006; Aysal *et al.* 2011). In contrast, the Pulur Massif and the Devrekani metamorphics are intruded by granites that are dated as Early Carboniferous (Topuz *et al.* 2007, 2010; Nzegge *et al.* 2006; T. Ustaömer & Robertson 2010).

In this paper, we report new Ion Probe U-Pb zircon age data from the Central Sakarya basement. We have dated detrital zircon grains from a sample of sillimanite-garnet-mica schist and igneous zircons from three cross-cutting granitoid intrusions.

Geological Setting of Dated Lithologies

The study area is located between the city of Bilecik in the west and the small town of Söğüt in the east (Figures 2 & 3). Pre-Jurassic basement and a Jurassic–Upper Cretaceous cover are well exposed along the Karasu and Sakarya rivers in this area (Altınlı 1973a, b; Demirkol 1977; Y. Yılmaz 1977, 1981; Saner 1978; Şentürk & Karaköse 1981; Kadıoğlu *et al.* 1994; Kibici 1991, 1999; Kibici *et al.* 2010; Duru *et al.* 2007). The Jurassic–Upper Cretaceous cover begins with Lower Jurassic coarse clastic sedimentary rocks (Bayırköy Formation), which pass gradually into Jurassic–Cretaceous neritic carbonates (Bilecik Limestone). The succession continues with diagenetic chert-bearing pelagic limestones and marls of Callovian–Aptian age (Soğukçam Formation). This unit is overlain by pelagic limestone, shale, volcanogenic sedimentary rocks and a turbiditic sequence that includes occasional debris-flow deposits of Albian–Late Palaeocene age (Yenipazar Formation; Duru *et al.* 2007). The clasts and blocks in the debris flow deposits are indicative of derivation from an ophiolitic source, plus the underlying Bilecik Limestone and its metamorphic basement. The Eocene is represented by unconformably overlying red continental clastic sedimentary rocks, limestones and marls.

Two different basement units are exposed unconformably beneath the Lower Jurassic cover units. The first, in the north, is an assemblage of paragneiss, schist and amphibolite, which is cut by granitoid intrusions (Göncüoğlu *et al.* 2000; Duru *et al.* 2002). This unit is termed the Central Sakarya basement and is the subject of this study (Ustaömer *et al.* 2010). The granitoid rocks (Figure 4) are also known as the Sarıcakaya granitoid (Göncüoğlu *et al.* 1996; Duru *et al.* 2007; Kibici *et al.* 2010), the Central Sakarya granite (O. Yılmaz 1979), the Söğüt magmatics (Kadıoğlu *et al.* 1994) and the Akçasu magmatics (Demirkol 1977). The paragneiss-schist and amphibolitic host rocks of the granitoid intrusions are also equivalent to the Söğüt metamorphics (Göncüoğlu *et al.* 1996, 2000; Şentürk & Karaköse 1979, 1981). The Söğüt metamorphics are mainly sillimanite-staurolite-garnet-bearing paragneiss, staurolite-bearing mica schists, muscovite-biotite schists, amphibolites, marble and quartz schists (Göncüoğlu *et al.* 2000). Lens-shaped bodies of cumulate metagabbro and meta-serpentinite also occur locally. The amphibolite facies metamorphic rocks are cut by grey and pink dykes and veins of granite, as exposed in the Küplü-Aşağıköy area (Figure 3) and the Akçasu and Sarıcakaya areas (to the NE of, but outside the study area).

The second type of basement unit in the area, of mainly greenschist or lower metamorphic grade, is correlated with the Triassic Nilüfer and Hodul units of the Karakaya Complex in the type area of the Biga Peninsula (Figure 2).

The contact of the Central Sakarya basement with the Karakaya Complex is a north-dipping mylonitic shear zone (Y. Yılmaz 1977; Kadıoğlu *et al.* 1994).

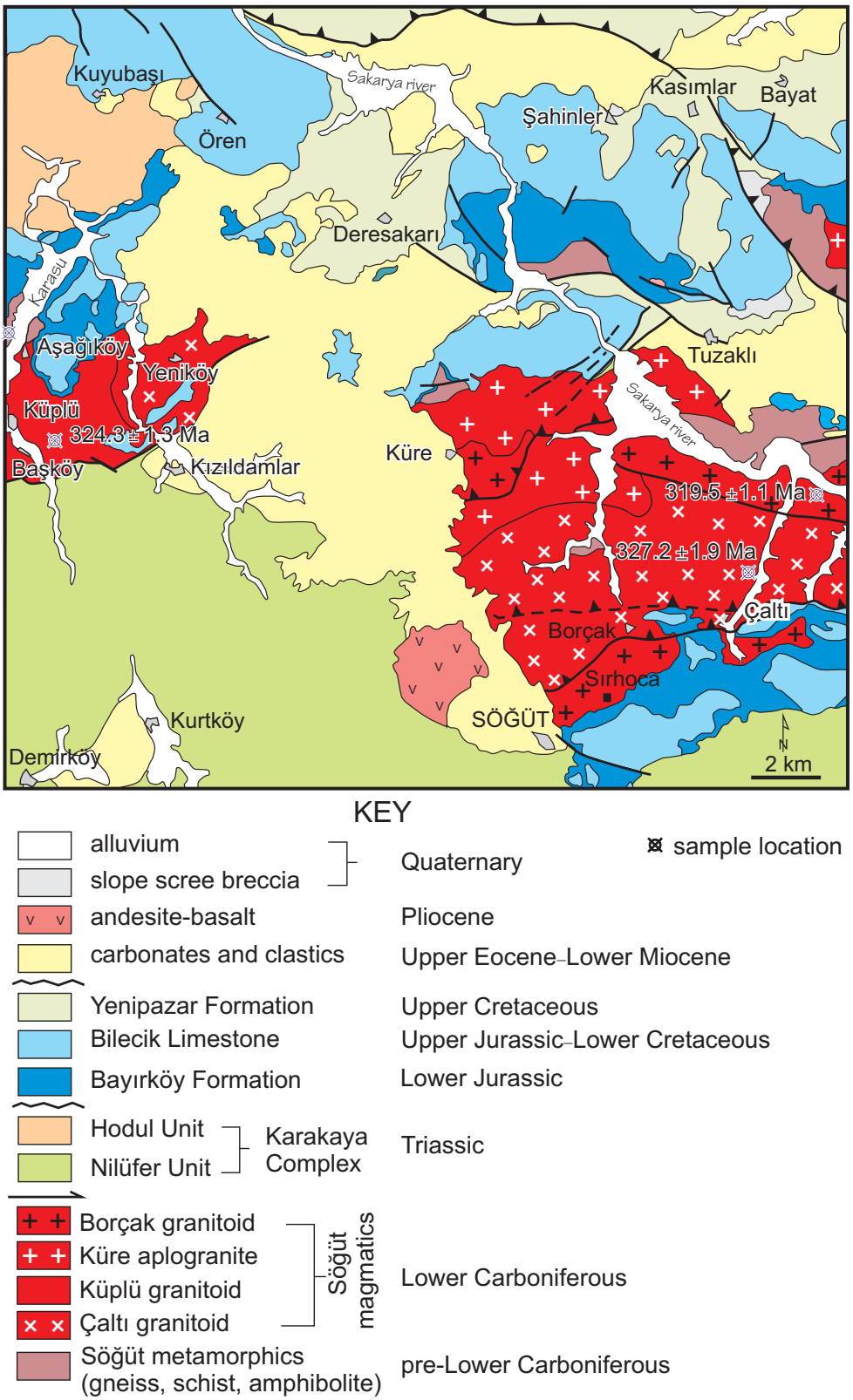

Figure 3. Geological map of the study area, compiled from Y. Yılmaz (1979), Kadıoğlu *et al.* (1994) and Duru *et al.* (2002, 2007).

Previous Work on the Sampled Units

Y. Yılmaz (1977) distinguished five mappable units of granitoid rocks in the Central Sakarya basement near Bilecik-Söğüt, based on field relations, petrographic and geochemical features (Figure 4). These are the Küre aplitic granite**,** the Hamitabat porphyritic microgranite, the Borçak granodiorite, the Çaltı gneissic granite and the Yeniköy migmatite. Kadıoğlu *et al.* (1994) similarly divided the granitoid into three mappable units (Figure 4). Both of these studies identified north-dipping tectonic contacts between the individual granitoid units. In contrast, more recent MTA mapping (Duru *et al.* 2007) depicted a single granitoid body, termed the Sarıcakaya granitoid.

Kadıoğlu *et al.* (1994) divided the Söğüt magmatics into three units in their study area north of Söğüt. From south to north, in structurally ascending order, these are the Sıraca granodiorite (equivalent to the Borçak granodiorite of Y. Yılmaz 1977), the Borçak granite (equivalent to the Çaltı gneissic granite of Y. Yılmaz 1977) and the Çaltı magmatics (equivalent to Yeniköy migmatite of Y. Yılmaz 1977). The Sıraca granodiorite is medium grained, with oligoclase + quartz + muscovite + sericite and minor amounts of biotite + actinolite + epidote + zircon + apatite + limonite. The Borçak granite is a well-foliated intrusion with quartz + oligoclase + orthoclase + muscovite + chloritised biotite + limonite. The Çaltı magmatics display compositional variation ranging from diorite-gabbro in the centre to granodiorite and granite at the margins. Various aplitic and pegmatitic dykes cut the Çaltı magmatics.

Based on major-element oxide analysis of a small number of samples, Kadıoğlu *et al.* (1994) inferred that the Söğüt magmatics are of calc-alkaline and S-type composition and that they were emplaced in a collisional setting. In contrast, Y. Yılmaz (1977) suggested an arc-type setting based on major-element oxide analysis, an interpretation that was supported by Göncüoğlu *et al.* (1996, 2000). Recently, Kibici *et al.* (2010) reported the results of a detailed major, trace and rare earth-element study of the Söğüt magmatics from around Sarıcakaya town in the east (outside our study area). The geochemistry of these rocks is indicative of a hybrid, arc-type/lower crustal origin. The authors infer that lower arc crust was underplated with subduction-related melts to form the granitoid intrusions.

Previously, Çoğulu *et al.* (1965) and Çoğulu & Krumennascher (1967) obtained U-Pb zircon evaporation and K/Ar biotite ages of 290 Ma and 290±5 Ma, respectively for the Söğüt magmatics. A.I. Okay *et al.* (2002) dated amphiboles from the granitoid using the Ar-Ar technique and obtained an age of 272±2 Ma.

Petrography of the Dated Samples

Çaltı Granitoid

The Çaltı granitoid is a granodiorite-tonalite made up of quartz + plagioclase + alkali feldspar + biotite ± chlorite ± opaque minerals. The rock fabric exhibits a preferred orientation characterised by an alignment of mica. Quartz was deformed under ductile conditions and reveals evidence of high-temperature grain-boundary migration. Large quartz crystals exhibit 'chessboard' patterns. Plagioclase is the dominant feldspar mineral and exhibits well-preserved magmatic zoning and mechanical twinning. The cores of the crystals are calcium-rich and more altered than their rims, which is attributed to low-temperature hydrothermal alteration. Sericitization is ubiquitous. Abundant reddish brown biotite is partly to completely chloritized. Biotite crystals commonly contain opaque mineral inclusions. Reddish brown biotite (iron-rich) is commonly replaced by chlorite with pale green or bluish green interference colours. An augen texture is developed with quartz and feldspars surrounded by micas. The fabric of the granitoid is interpreted to have resulted from high-temperature deformation within a relatively low-strain stress environment.

Küplü Granitoid

The Küplü granitoid is made up of quartz + alkali feldspar + plagioclase + hornblende ± biotite ± chlorite ± epidote ± sericite ± calcite ± opaque. The crystal size is finer than in the Çaltı granitoid and deformation is more intense. Quartz is almost completely recrystallized so that any pre-existing chessboard pattern was destroyed. Some feldspars are also recrystallized. Plagioclase crystals exhibit

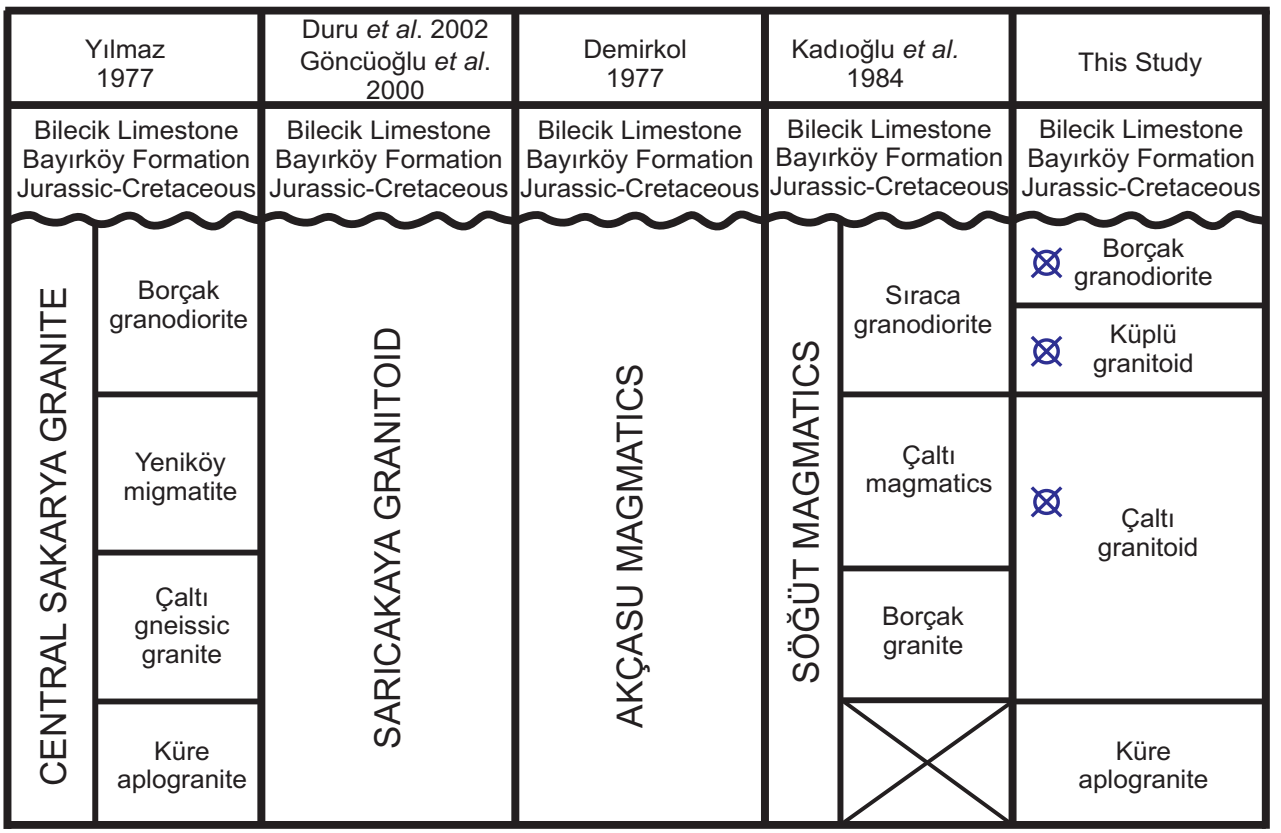

Figure 4. Subdivisions of the Söğüt magmatics according to different authors. See text for further information.

a magmatic zonation and deformation twins are quite common. Albite-pericline twins occur locally. Primary magmatic features are preserved despite the high-temperature deformation. The epidote, calcite and sericite resulted from low-temperature hydrothermal alteration.

Borçak Granitoid

The Borçak granitoid is a granodiorite composed of quartz + alkali feldspar + plagioclase + biotite + hornblende ± epidote ± sericite ± opaque minerals. Quartz is well preserved and shows a chessboard pattern. Quartz is deformed by grain-boundary migration, similar to the Çaltı granitoid. A penetrative fabric (e.g., foliation) is absent, in contrast to the two granitic bodies described above. Plagioclase exhibits deformation twins. The crystal cores are strongly altered whereas the rims are less altered. The main mafic minerals present are biotite and amphibole. The biotite is locally deformed with the development, for example, of kink banding.

Sillimanite-Garnet Schist

The host rock of the Küplü granitoid is made up of quartz + mica (biotite and muscovite) + garnet + feldspars + sillimanite. Quartz crystals again exhibit chessboard deformation. Primary staurolite is pseudomorphed by muscovite. Secondary rosette-shaped biotite crystals are likely to have formed in response to contact metamorphism. Biotite is commonly replaced by white mica, which is indicative of retrograde metamorphism. Fine-grained sillimanite fibres are intergrown with biotite.

U-Pb Zircon Dating

Three samples of granitoid rocks from the Central Sakarya basement and one sample from the host

schists were selected for dating. Zircons were separated from the samples using standard methods (i.e. crushing, milling, magnetic separation, heavy liquid separation and hand-picking under a binocular microscope). One hundred zircon grains were separated from the schist sample, eighty-nine of which were analysed.

Ion Microprobe Analytical Method

The U/Pb ion probe dating of the zircons was carried using a CAMECA ims-1270 ion microprobe at the Edinburgh Ion Microprobe Facility (EIMF), in the Material and Micro-Analysis Centre (EMMAC) of the School of GeoSciences, University of Edinburgh (UK). The zircons were analysed using a ~4–7nA O_2^- primary ion source with 22.5 keV net impact energy. The beam was focused using Köhler illumination (~25 μm maximum dimension) giving sharp edges and flat bottom pits. The effects of peripheral contamination were minimised by a field aperture that restricted the secondary ion signal to a ~15 μm square at the centre of the analysis pit.

A 60 eV energy window was used together with mass spectrometer slit widths to achieve a measured mass resolution of >4000R (at 1% peak height). Oxygen flooding on the surface of the sample increased the Pb ion yield by approximately a factor of two compared to non-flooding conditions. Prior to measurement, a 15-μm raster was applied on the sample surface for 120 seconds to remove any surface contamination around the point of analysis (total diameter of cleaned area ~40 μm).

The calibration of Pb/U ratios followed procedures employed by SIMS dating facilities elsewhere (SHRIMP or Cameca ims-1270). This is based on the observed relationship between Pb/U and the ratios of uranium oxides to elemental uranium (e.g., Compston *et al.* 1984; Williams & Claesson 1987; Schuhmacher *et al.* 1994; Whitehouse *et al.* 1997; Williams 1998). However, as noted by Compston (2004) the addition of UO_2 can improve the precision of measurement. The relationship between ln(Pb/U) vs. ln(UO_2/UO) is employed in preference to the conventional ln(Pb/U) vs ln(UO/U) or ln(Pb/U) vs ln(UO_2/U) methods and results in an increased within-session reproducibility of our own analyses of the standard by approximately a factor of two. A slope factor for ln(Pb/U) vs ln(UO_2/UO) of 2.6 was used for all zircon calibrations.

U/Pb ratios were calibrated against measurements of the Geostandards 91500 zircon (Wiedenbeck *et al.* 1995: ~1062.5 Ma; assumed $^{206}Pb/^{238}U$ ratio= 0.17917), which is measured after each three to four unknowns. Measurements over a single 'session' (a period in which no tuning or changes to the instrument took place) give a standard deviation on the $^{206}Pb/^{238}U$ ratio of individual repeats of 91500 of about 1% (1s). Fast analyses using a secondary standard (Temora-2) were performed and the same age (within error) is obtained.

Th/U ratios in unknown zircons were calculated by reference to measurements of Th/U and $^{208}Pb/^{206}Pb$ on the 91500 standard, assuming closed system behaviour. Element concentrations were determined based on observed oxide ratios of the standard (UO_2/Zr_2O_2 and HfO/Zr_2O_2; assuming U= 81.2 ppm, Hf = 5880 ppm).

Common Pb contribution to analyses is primarily assumed to result from surface contamination of the sample by modern-day common Pb. A correction for a mass fractionation of 2‰ /mass unit was initially made, followed by a linear correction for the intensity of drift on all masses with time. To further reduce possible near-surface contamination of common Pb (following exclusion of the first five cycles through the masses) the average ratios were calculated from the remaining 15 cycles. The total time for each analysis was approximately 27 minutes.

The uncertainty of the Pb/U ratio includes an error based on the observed uncertainty from each measured ratio. This is generally close to that expected from counting statistics. However, observed uncertainty of the U/Pb ratio of the standard zircon is generally an additional 0.8% in excess of that expected from counting statistics, alone. This is assumed to be a random error (see Ireland & Williams 2003) that has been propagated in both standards and unknowns together with the observed variation in Pb/U ratios measured for each analysis (typically close to the counting errors). Uncertainties on ages quoted in the text and in tables for individual analyses (ratios and ages) are at the 1s level. Plots and age calculations have been made using the computer program ISOPLOT/EX v3 (Ludwig 2003).

In the exploration, or fast analysis, mode (7 minute analyses) the pre-sputter was limited to 60 seconds and measurements were limited to peaks for Zr_2O, all four lead isotopes, plus ThO_2 and UO_2. Only 8 cycles were measured and no cycles were excluded. Approximately 10 unknowns were run between each measurement of the 91500 standard. U/Pb ratios were determined using Pb/UO_2 alone and assumed constant primary and secondary beam conditions between each measurement of the standard. In reality the Pb/UO_2 ratios were sufficiently stable that unknowns could be compared to the average of all standards run over two separate analytical sessions. Whilst counting errors for the U/Pb ratio were generally between 0.5 and 1.0%, the reproducibility of the standard was approximately 1.0% in excess of that expected and the uncertainty quoted for the unknown. The ThO_2/UO_2 ratios were used to determine Th/U ratios assuming a closed system behaviour of the combined 91500 standards. The average measured ThO_2/UO_2 ratio for the 91500 standard was within 2% of the Th/U ratio calculated from the measured $^{208}Pb/^{206}Pb$ ratios (and the known age of the standard). Common lead was corrected where the measured ^{204}Pb exceeded three counts: ^{204}Pb measured was generally <4 ppb.

Results

Metasedimentary Rock

The detrital zircons that were separated from the metasedimentary schist are mostly colourless, although some are brown or reddish. Most of the zircons are subhedral but a few are euhedral or well rounded. Internal structures are variable, as revealed by cathodoluminiscence (CL) images (Figure 5). Most of the zircon grains display oscillatory zoning, typical of igneous zircons. The analysed Th/U ratios of the zircons are > 0.1, consistent with an igneous origin. A single zircon has a Th/U ratio of 0.01, suggestive of a metamorphic origin (Teipel *et al.* 2004).

The resulting ion-probe U-Pb ages of eighty-nine detrital zircons that were analysed range from 551 Ma (Ediacaran) to 2738 Ma (Neoarchean) (Table 1). Eighty five percent of the ages are 90–110% concordant. Zircon populations cluster at ~550–750 Ma (28 grains), ~950–1050 Ma (27 grains) and ~2000 Ma (5 grains), with smaller groupings at ~800 Ma and ~1850 Ma (Figure 5). The youngest concordant zircon age is 551 Ma (Figure 6).

Magmatic Rocks

Euhedral zircons from the three intrusions show marked internal differences. In particular, the zircons from the Borçak granitoid sample show wider oscillation bands (Figure 7a) than those from the Küplü granitoid (Figure 7b). In contrast, the zircons from the Çaltı metagranitoid exhibit inherited cores that are rimmed by fine oscillatory zoned domains (Figure 7c). The rims are relatively dark compared to those from the Küplü granitoid.

The Çaltı granitoid is dated at 327.2±1.9 Ma (Figure 8a, Table 2). The inherited core ages are mostly discordant except for one that is 99% concordant (482 Ma; Tremadocian). The Küplü granitoid yielded a slightly younger age of 324.3±1.5 Ma (Figure 8b, Table 2), compared to the Çaltı granitoid. The Borçak granitoid, in contrast, yielded a significantly younger age of 319.5±1.1 Ma (Figure 8c, Table 2). The granitoid bodies, therefore, appear to have been emplaced over approximately eight million years during late Early Carboniferous (Visean to Serpukhovian) time.

Discussion

Age of the Central Sakarya Basement

The morphologies of the zircons separated from the dated metasedimentary rocks (Figure 5) are significant for an interpretation of the age results. Some of these are well-rounded to sub-rounded, suggesting prolonged sedimentary transport. The internal structure of these zircons is homogenous, patchy and weakly zoned. Thin oscillatory rims are seen in some of these grains (Figure 5). Many of the well-rounded zircons gave ages of 0.95 to 1.05 Ga, whereas some of the other well-rounded grains gave ages of ~0.75 Ga and 1.7 Ga. In addition, the sub-rounded zircons gave ages mainly between 0.6 and 0.7 Ga, with some from 1.8 to 2.2 Ga and a few from 0.8 to 1.2 Ga. In contrast, a third group of mostly euhedral zircons yielded ages of 0.68 to 0.7 Ga and 1.8 to 2.1 Ga. The euhedral shape is consistent with a relatively local source without prolonged sedimentary

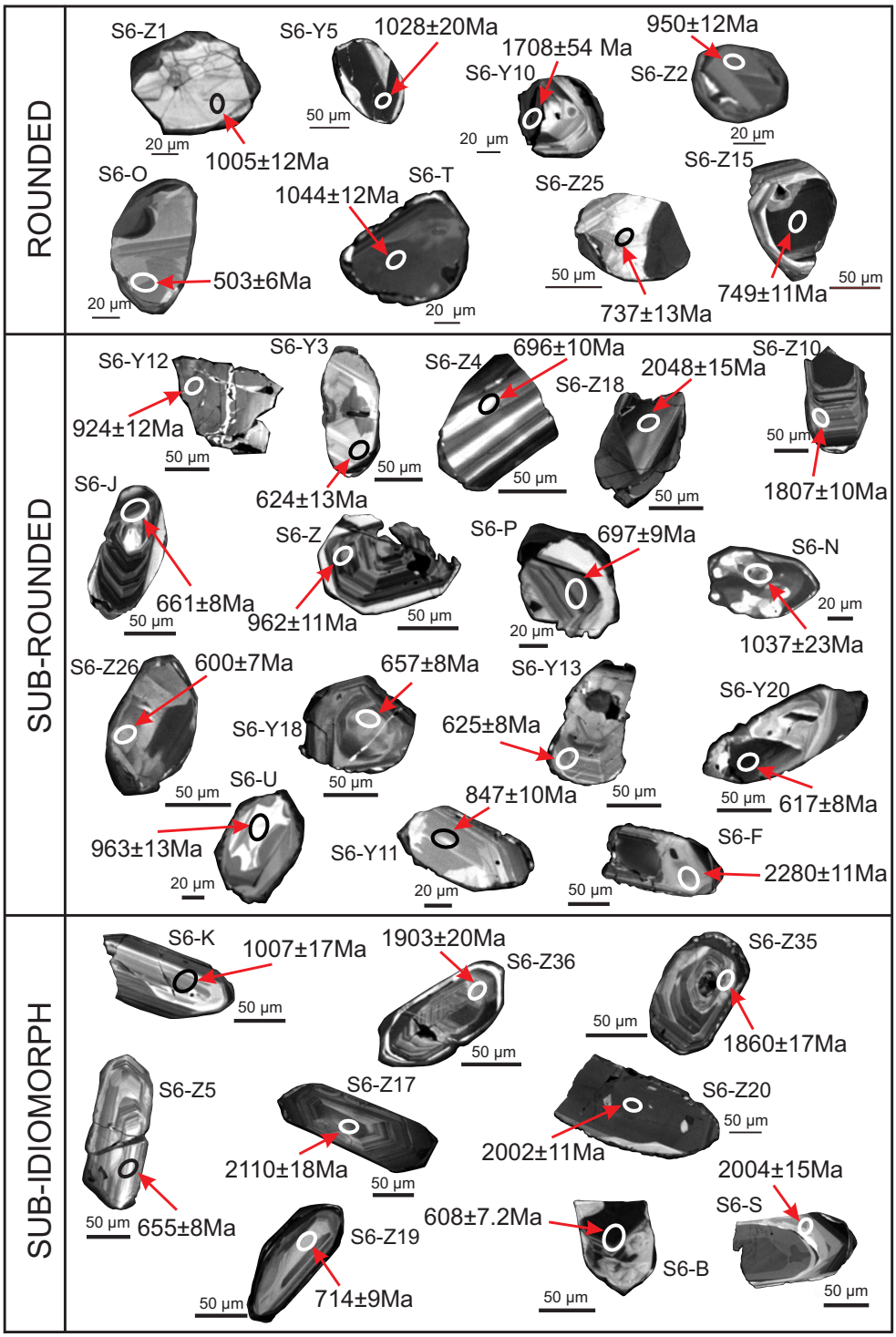

Figure 5. Selected cathodoluminescence images of the zircon grains analysed from the country rock schist sample. The zircons fall into three groups based on degree of roundness. Locations of the Ion Probe analysis spots and the corresponding ages are indicated. Note that the Kibaran-aged zircons (0.9–1.1 Ga) form the most prominent population in the groups of well-rounded and sub-rounded grains. $^{206}Pb/^{238}U$ is used for ages < 1000 Ma and $^{207}Pb/^{206}U$ for > 1000 Ma in constructing the diagram. See text for discussion.

Table 1. U/Pb isotope ratios of detrital zircons from the sillimanite-garnet schist sample in the study area. GPS location of the dated sample: 02444576 4445760.

										apparent age (Ma)				
L-No.	U (ppm)	Th (ppm)	Pb (ppm)	Th/U	$^{206}Pb/^{238}U$	±1σ (%)	$^{207}Pb/^{235}U$	±1σ (%)	Rho	$^{206}Pb/^{238}U$	±1σ	$^{207}Pb/^{235}U$	$^{207}Pb/^{206}Pb$	±1σ
a	792.3	305	123.4	0.395	0.1799	0.0021	1.8659	0.0312	0.6908	1066	12.3	1068	1074	24
b	767.2	5	65.7	0.007	0.0990	0.0012	0.8517	0.0159	0.6367	608	7.2	625	688	31
d	64.3	44	6.6	0.705	0.1180	0.0016	1.0751	0.0486	0.3046	719	9.9	741	809	90
e	863.1	355	82.7	0.422	0.1108	0.0013	0.9441	0.0163	0.6793	677	8.0	675	668	27
f	1195.5	188	361.3	0.161	0.3492	0.0050	6.9516	0.1095	0.9088	1931	27.6	2104	2280	11
g	144.5	53	11.6	0.377	0.0931	0.0012	0.7651	0.0218	0.4590	574	7.5	577	588	54
i	90.9	64	14.0	0.728	0.1678	0.0020	1.6975	0.0558	0.3646	1000	12.0	1007	1023	62
j	53.2	36	21.6	0.554	0.1080	0.0014	0.8960	0.0176	0.6439	661	8.3	649	610	32
k	165.3	142	24.4	0.754	0.1754	0.0022	1.7590	0.0272	0.8070	1042	13.0	1030	1007	17
l	90.9	64	14.0	0.725	0.1776	0.0029	1.7370	0.0618	0.4586	1054	17.2	1022	954	64
m	53.2	36	21.6	0.696	0.4698	0.0058	10.8586	0.1943	0.6866	2483	30.5	2509	2534	22
n	165.3	142	24.4	0.883	0.1709	0.0020	1.7404	0.0285	0.7177	1017	12.0	1023	1037	23
o	655.5	21	46.0	0.033	0.0811	0.0009	0.6676	0.0101	0.7711	503	5.8	519	593	21
p	247.5	129	24.5	0.536	0.1142	0.0014	1.0173	0.0337	0.3785	697	8.7	712	761	64
q	231.6	118	32.7	0.522	0.1631	0.0022	1.6000	0.0303	0.7105	974	13.1	970	961	26
r	203.4	77	21.6	0.388	0.1227	0.0015	1.1301	0.0350	0.4023	746	9.3	767	831	59
s	302.7	151	93.9	0.512	0.3585	0.0041	6.0944	0.0862	0.8165	1975	22.8	1988	2004	15
t	390.4	173	59.4	0.454	0.1759	0.0020	1.7584	0.0285	0.7150	1044	12.1	1030	1000	23
u	79.6	43	11.1	0.558	0.1612	0.0022	1.5639	0.0443	0.4860	963	13.3	955	939	51
v	79.6	87	12.1	1.117	0.1756	0.0025	1.8258	0.0590	0.4468	1043	15.1	1054	1079	58
y	158.1	113	21.0	0.731	0.1534	0.0018	1.5198	0.0295	0.6056	920	10.8	938	982	31
z	202.8	165	28.3	0.835	0.1610	0.0019	1.5723	0.0370	0.4985	962	11.3	959	952	42
z1	154.4	72	22.5	0.481	0.1687	0.0020	1.6733	0.0464	0.4336	1005	12.1	998	984	51
z2	255.9	145	35.2	0.579	0.1587	0.0019	1.4983	0.0348	0.5239	950	11.5	929	882	41
z3	173.3	104	70.1	0.614	0.4675	0.0056	11.5208	0.1693	0.8090	2473	29.4	2565	2640	14
z4	196.8	113	19.4	0.590	0.1140	0.0016	0.9335	0.0323	0.4018	696	9.7	669	582	65
z5	208.5	210	19.3	1.034	0.1069	0.0013	0.9327	0.0288	0.3938	655	8.0	669	717	60
z6	26.9	14	3.1	0.551	0.1322	0.0024	1.2643	0.1041	0.2188	800	14.4	829	909	165

Table 1. Continued.

										apparent age (Ma)				
L-No.	U (ppm)	Th (ppm)	Pb (ppm)	Th/U	$^{206}Pb/^{238}U$	±1σ (%)	$^{207}Pb/^{235}U$	±1σ (%)	Rho	$^{206}Pb/^{238}U$	±1σ	$^{207}Pb/^{235}U$	$^{207}Pb/^{206}Pb$	±1σ
z7	787.7	215	88.7	0.281	0.1302	0.0015	1.2079	0.0165	0.8481	789	9.2	804	847	15
z8	542.8	187	106.5	0.354	0.2266	0.0029	2.6698	0.0378	0.9126	1317	17.0	1319	1325	11
z9	311.2	269	47.0	0.887	0.1744	0.0020	1.7419	0.0290	0.6966	1036	12.0	1024	997	24
z10	1224.8	44	326.6	0.037	0.3080	0.0043	4.6920	0.0700	0.9335	1731	24.1	1765	1807	10
z11	36.3	23	3.6	0.652	0.1133	0.0018	0.9971	0.0831	0.1900	692	11.0	702	735	169
z12	129.1	92	40.0	0.730	0.3579	0.0047	6.0625	0.1125	0.7070	1972	25.9	1984	1997	23
z13	368.4	334.1	38.5	0.930	0.1207	0.0014	1.0690	0.0152	0.8250	735	8.6	738	749	17
z14	507.3	770.4	40.6	1.558	0.0924	0.0013	0.7517	0.0154	0.6710	570	7.8	569	566	33
z15	191.7	125.1	20.4	0.669	0.1231	0.0018	1.0920	0.0301	0.5414	749	11.2	749	751	49
z16	272.0	138.2	21.4	0.521	0.0909	0.0011	0.7346	0.0186	0.4702	561	6.7	559	553	49
z17	184.3	81.0	61.8	0.451	0.3872	0.0045	6.9919	0.1080	0.7579	2110	24.7	2109	2110	18
z18	101.7	50.8	32.3	0.512	0.3667	0.0045	6.3918	0.0965	0.8052	2014	24.5	2030	2048	15
z19	356.0	118.0	36.1	0.340	0.1172	0.0014	1.0392	0.0232	0.5364	714	8.6	723	751	40
z20	303.9	274.7	89.0	0.927	0.3382	0.0039	5.7452	0.0750	0.8738	1878	21.4	1937	2002	11
z21	187.3	145.2	15.0	0.795	0.0923	0.0013	0.7453	0.0234	0.4446	569	7.9	565	549	61
z22	424.0	634.5	34.2	1.535	0.0932	0.0011	0.7789	0.0158	0.6022	574	7.0	584	626	35
z23	171.1	60.2	15.6	0.361	0.1050	0.0013	0.8378	0.0275	0.3792	644	8.0	618	524	65
z24	138.6	51.7	19.8	0.382	0.1650	0.0021	1.6362	0.0487	0.4245	985	12.4	984	983	54
z25	49.5	21.3	5.2	0.442	0.1211	0.0021	1.1179	0.0469	0.4213	737	13.0	761	836	72
z26	325.3	4.2	27.4	0.013	0.0975	0.0012	0.8140	0.0148	0.6786	600	7.4	604	623	29
z27	62.5	137.3	8.1	2.253	0.1498	0.0023	1.5043	0.0575	0.3992	900	13.7	932	1008	70
z28	85.8	114.8	7.4	1.373	0.1002	0.0013	0.8368	0.0257	0.4145	615	7.8	617	624	57
z29	119.8	78.6	33.3	0.673	0.3209	0.0043	5.1209	0.0946	0.7332	1794	24.3	1838	1891	23
z30	175.0	79.0	75.1	0.463	0.4962	0.0059	12.5773	0.1812	0.8210	2597	30.7	2647	2687	14
z31	104.2	28.8	15.4	0.284	0.1713	0.0021	1.7260	0.0603	0.3555	1019	12.7	1018	1015	62
z32	350.9	11.4	31.6	0.033	0.1040	0.0013	0.8678	0.0131	0.8056	638	7.8	634	621	19
z33	287.5	179.6	29.3	0.641	0.1176	0.0014	1.0059	0.0174	0.6914	717	8.6	706	675	27
z34	173.2	60	50.5	0.353	0.3372	0.0041	7.3386	0.1031	0.8669	1873	22.8	2152	2432	12
z35	108.7	99	31.4	0.937	0.3336	0.0039	5.2332	0.0796	0.7787	1856	22.0	1857	1860	17

Table 1. Continued.

										apparent age (Ma)				
L-No.	U (ppm)	Th (ppm)	Pb (ppm)	Th/U	$^{206}Pb/^{238}U$	±1σ (%)	$^{207}Pb/^{235}U$	±1σ (%)	Rho	$^{206}Pb/^{238}U$	±1σ	$^{207}Pb/^{235}U$	$^{207}Pb/^{206}Pb$	±1σ
z36	246.7	245	71.6	1.017	0.3353	0.0039	5.3849	0.0869	0.7123	1864	21.4	1881	1903	20
z37	116.4	142	10.2	1.248	0.1010	0.0014	0.8477	0.0237	0.5075	620	8.8	623	634	52
z38	57.4	28	8.7	0.502	0.1756	0.0024	1.8006	0.0640	0.3912	1043	14.5	1045	1051	65
z39	151.2	98	21.6	0.665	0.1651	0.0023	1.6458	0.0362	0.6407	985	13.9	987	994	34
z41	240.0	142	74.5	0.607	0.3587	0.0042	8.5113	0.1168	0.8517	1976	23.1	2286	2577	12
z42	338.3	177	56.0	0.538	0.1911	0.0023	2.0214	0.0383	0.6321	1127	13.5	1122	1114	29
z43	50.1	15	18.8	0.314	0.4326	0.0053	10.6211	0.2103	0.6180	2317	28.3	2489	2635	26
z44	125.3	96	39.1	0.783	0.3608	0.0048	6.2253	0.1281	0.6493	1986	26.5	2007	2030	27
z45	543.0	203	48.2	0.384	0.1025	0.0012	0.8363	0.0174	0.5640	629	7.4	617	573	36
z46	16.6	5	1.6	0.307	0.1132	0.0023	1.0041	0.1206	0.1713	692	14.2	705	751	222
z47	128.5	96	17.1	0.765	0.1538	0.0022	1.5592	0.0706	0.3093	922	12.9	954	1028	87
z48	117.6	63	11.4	0.549	0.1115	0.0017	0.9922	0.0409	0.3631	681	10.2	699	760	81
y1	135.9	169	20.5	1.278	0.1739	0.0021	1.7809	0.0621	0.3387	1033	12.2	1038	1049	65
y2	472.9	204	213.8	0.442	0.5222	0.0061	13.6507	0.1696	0.9433	2708	31.7	2724	2738	7
y3	110.8	161	9.8	1.488	0.1016	0.0021	0.8640	0.0854	0.2046	624	12.6	632	661	155
y4	300.9	10	29.8	0.034	0.1143	0.0016	0.9695	0.0305	0.4465	698	9.8	688	657	59
y5	849.7	616	130.0	0.744	0.1768	0.0020	1.7924	0.0270	0.7554	1049	11.9	1042	1028	20
y6	757.4	124	104.0	0.167	0.1587	0.0019	1.5782	0.0266	0.7208	950	11.6	961	989	23
y7	72.6	42	8.6	0.595	0.1368	0.0021	1.3165	0.0513	0.3892	826	12.5	852	922	64
y8	145.2	105	18.6	0.739	0.1480	0.0019	1.5033	0.0637	0.2952	889	11.1	931	1033	82
y9	152.7	114	21.4	0.769	0.1618	0.0022	1.5508	0.0487	0.4391	967	13.3	950	914	52
y10	164.1	75	42.6	0.469	0.2998	0.0058	4.3272	0.1534	0.5483	1690	32.8	1697	1708	54
y11	117.1	49	14.2	0.432	0.1403	0.0017	1.3144	0.0517	0.3116	847	10.4	852	866	77
y12	184.9	84	24.7	0.466	0.1541	0.0019	1.5264	0.0425	0.4493	924	11.6	940	981	48
y13	193.4	135	17.0	0.714	0.1018	0.0013	0.8572	0.0293	0.3639	625	7.8	628	642	68
y14	27.9	1184	2.5	43.582	0.1029	0.0022	1.0722	0.0833	0.2701	631	13.2	739	1083	150
y15	241.2	229	60.4	0.973	0.2891	0.0036	4.5377	0.0693	0.8239	1637	20.6	1737	1861	15
y16	953.1	120	92.4	0.129	0.1120	0.0013	0.9672	0.0161	0.7194	684	8.2	687	696	23
y17	254.3	115	38.0	0.466	0.1726	0.0022	1.7938	0.0373	0.6143	1026	13.1	1043	1078	33
y18	488.1	333	45.3	0.701	0.1073	0.0014	0.9022	0.0188	0.6043	657	8.3	652	638	36
y19	967.6	470	74.7	0.498	0.0892	0.0010	0.7137	0.0174	0.4776	551	6.4	547	530	46
y20	337.3	398	29.3	1.210	0.1004	0.0012	0.8478	0.0179	0.5797	617	7.5	623	648	36

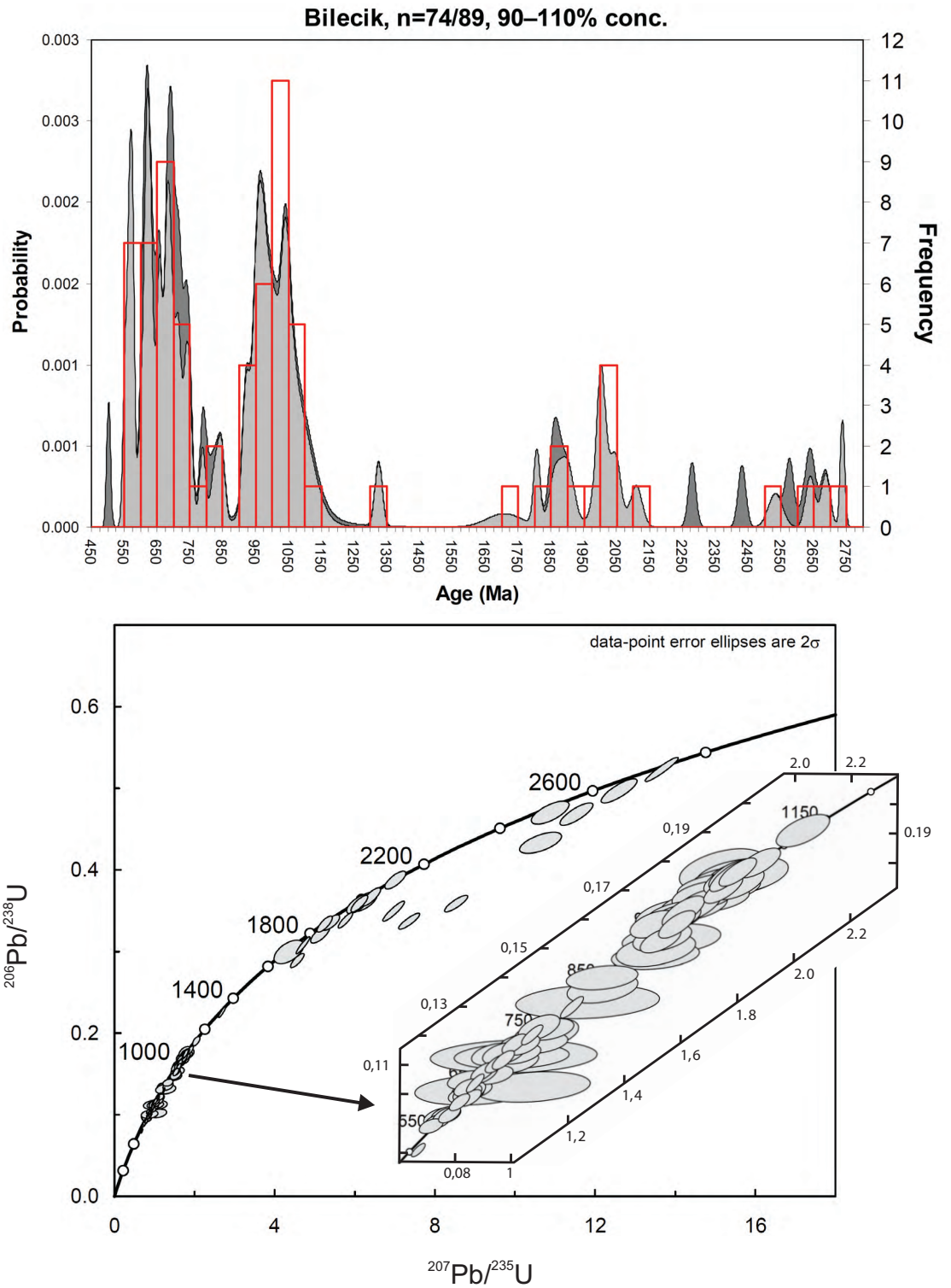

Figure 6. Probability density distribution (upper) and concordia diagram (lower) of the detrital zircon ages obtained during this study from the country rock schist sample. See text for discussion. The dark grey field on the probability density distribution diagram shows the discordant ages. $^{206}Pb/^{238}U$ is used for ages < 1000 Ma and $^{207}Pb/^{206}U$ for > 1000 Ma in constructing the diagram.

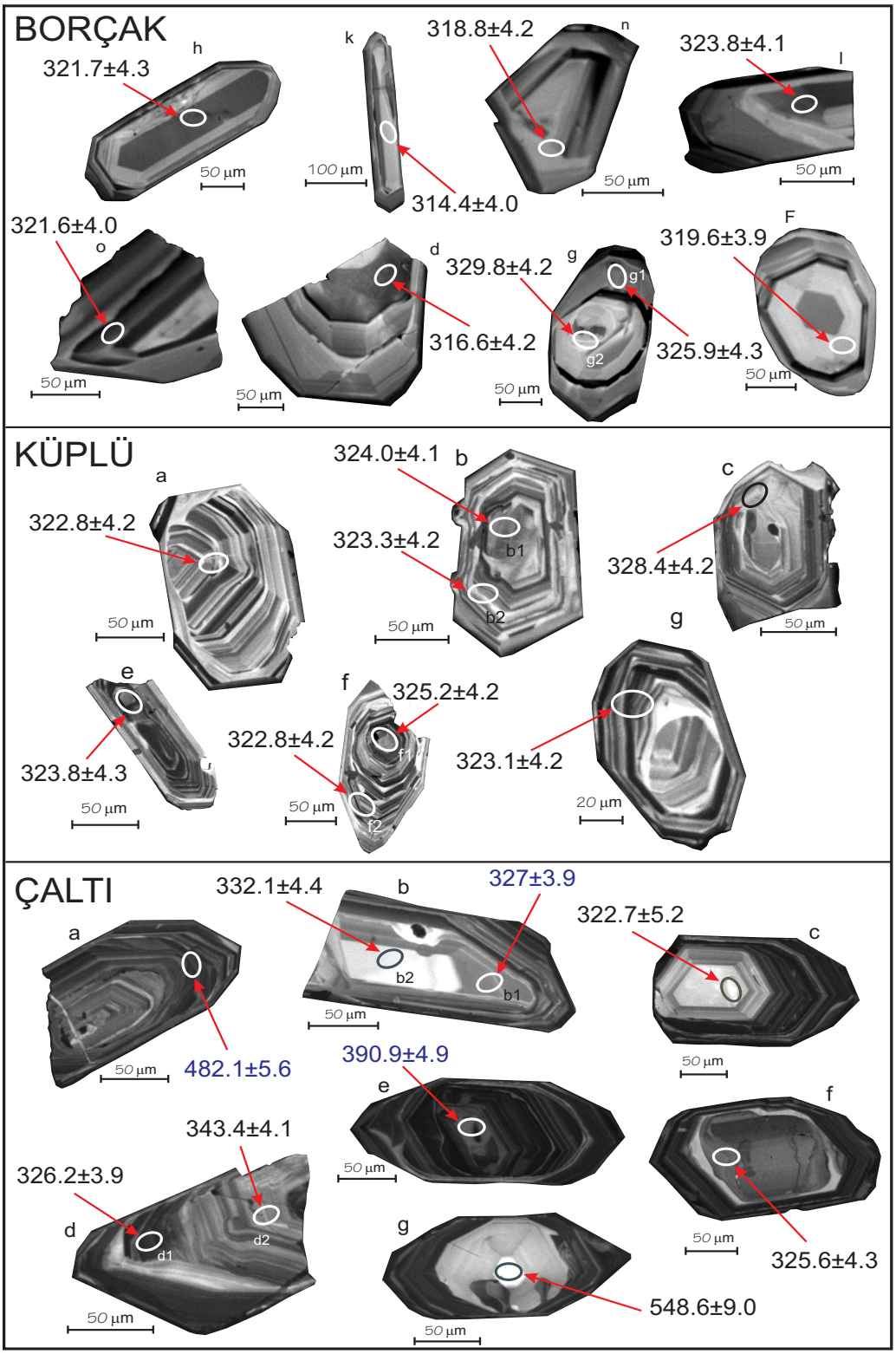

Figure 7. Selected cathodoluminescence images of zircons analysed from the granitoids. Location of the Ion Probe analysis spots and the corresponding ages are also indicated. **(a)** Borçak, **(b)** Küplü and **(c)** Çaltı metagranitoids.

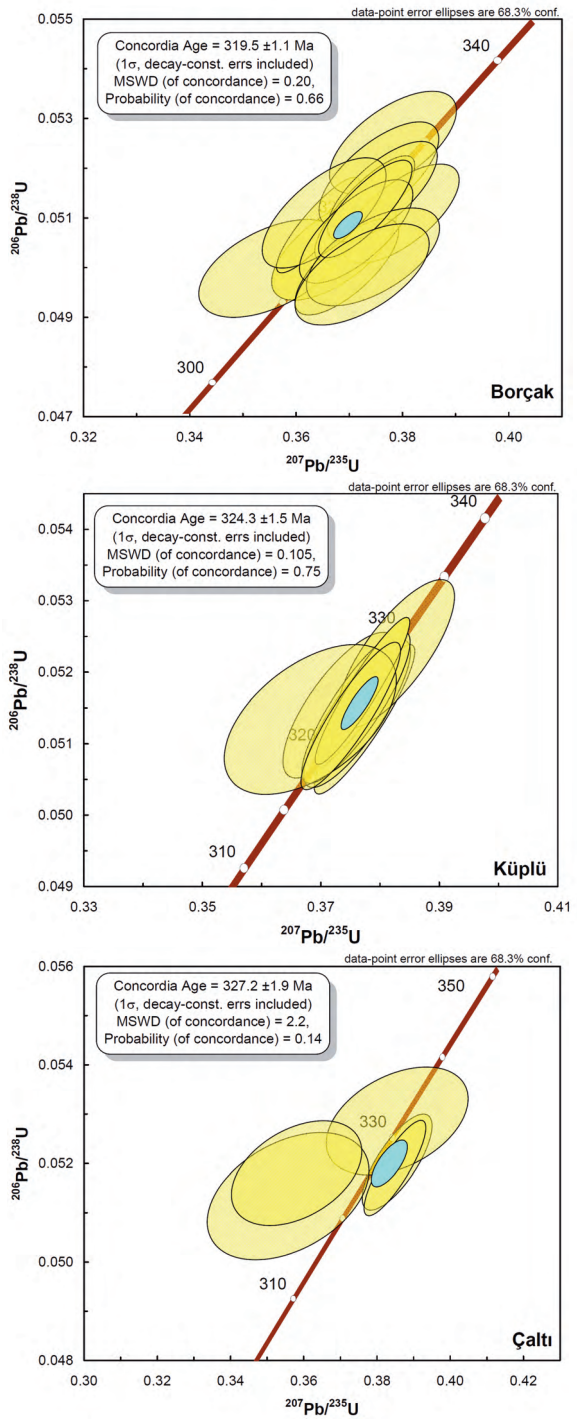

Figure 8. Concordia diagrams of Borçak, Küplü and Çaltı metagranitoids. See text for discussion.

transport. The zircons in this group commonly display concentric oscillatory zoning although patchy and homogenous varieties also occur (Figure 5).

The maximum depositional age of the metasedimentary rock is 551 Ma, based on the concordant age of the youngest zircon in the sample. The 327 Ma (Visean) age of the oldest zircons from the granitoid sample further constrains the age of deposition as between Ediacaran (551 Ma) and Visean (327 Ma); i.e. probably Early Palaeozoic.

The possible source area of the metasedimentary rock can be inferred by comparison with the reported ages of major cratons and peri-Gondwanian terranes. In Figure 9, the source ages of major cratons are placed to the left, the North African basins in the middle, while several Peri-Gondwanan terranes are shown to the right of the diagram. Our detrital zircon data are shown to the right for comparison.

In our data the most prominent population is of late Neoproterozoic age. This suggests derivation from a Gondwana-related source area, either related to the Cadomian-Avalonian magmatic arc, from 550–650 Ma, or from within the East African orogen (equivalent to the Mozambique belt; Stern 1994) from 550–850 Ma (Nance *et al.* 2008). Several alternative potential source areas were not magmatically active during these time periods. Specifically, Baltica and Siberia (equivalent to Angara) are not believed to have been magmatically active during the late Neoproterozoic (Meert & van der Voo 1997; Greiling *et al.* 1999; Hartz & Torsvik 2003; Meert & Torsvik 2003; Murphy *et al.* 2004a, b; Sunal *et al.* 2006; see Figure 9). The Avalonian terranes, additional potential source regions, are characterised by Mesoproterozoic ages (Figure 9; Nance & Murphy 1994; Winchester *et al.* 2006). However, the absence of 1.2–1.6 Ga ages in our data set makes an Avalonian affinity unlikely.

The second largest population in our data set is early Neoproterozoic (0.9–1.0 Ga). Cadomian terranes are characterised by a reported absence of Grenvillian ages (Fernández-Suarez *et al.* 2002; Gutiérrez-Alonso *et al.* 2003). The presence of Kibaran or Grenvillian aged zircons in our data set, therefore, differs significantly from the known age ranges of Cadomian terranes (e.g., Armorican Terrane Assemblage; Figure 9).

An alternative is a source within the Arabian-Nubian shield of northeast Gondwana. This more probable because the 'Minoan terranes' that are believed to have originated from the Arabian-

Table 2. U/Pb isotope ratios of zircons from magmatic rocks in the study area. * denotes the core analyses which are not used in construction of the concordia diagram for the Çaltı granitoid. GPS locations of the dated samples: Küplü granitoid: 0245609 4442634; Borçak granitoid: 0267762 4440486; Çaltı granitoid: 0266100 4437998.

Sample	L-No.	U (ppm)	Th (ppm)	Pb (ppm)	$\frac{Th}{U}$	$\frac{^{206}Pb}{^{238}U}$	±1σ (%)	$\frac{^{207}Pb}{^{235}U}$	±1σ (%)	Rho	apparent age (Ma) $\frac{^{206}Pb}{^{238}U}$	±1σ	$\frac{^{207}Pb}{^{235}U}$	±1σ
Çaltı granitoid	a*	516.8	18.4	37.1	0.037	0.6062	0.0076	0.0776	0.0009	0.9535	482.1	5.6	481.1	4.8
Çaltı granitoid	b1	202.0	61.0	10.5	0.310	0.3853	0.0063	0.0520	0.0006	0.7541	327.0	3.9	330.9	4.6
Çaltı granitoid	b2	30.8	28.0	1.9	0.934	0.3853	0.0128	0.0529	0.0007	0.4098	332.1	4.4	330.9	9.3
Çaltı granitoid	e*	192.5	42.5	11.7	0.227	0.4835	0.0074	0.0625	0.0008	0.8438	390.9	4.9	400.5	5.0
Çaltı granitoid	g*	190.7	33.1	16.3	0.178	0.7348	0.0142	0.0888	0.0015	0.8796	548.6	9.0	559.4	8.3
Çaltı granitoid	d1	307.2	42.7	15.2	0.143	0.3847	0.0056	0.0519	0.0006	0.8444	326.2	3.9	330.5	4.1
Çaltı granitoid	c	43.6	20.6	2.3	0.485	0.3554	0.0146	0.0513	0.0009	0.4027	322.7	5.2	308.8	10.9
Çaltı granitoid	d2*	945.8	156.8	49.5	0.170	0.3958	0.0055	0.0547	0.0007	0.8832	343.4	4.1	338.6	4.0
Çaltı granitoid	f	60.5	45.3	3.5	0.769	0.3578	0.0118	0.0518	0.0007	0.4102	325.6	4.3	310.5	8.8
Küplü granitoid	a	335.2	120.3	17.4	0.368	0.0513	0.0007	0.3773	0.0056	0.9046	322.8	4.2	325.0	4.1
Küplü granitoid	br	258.5	81.2	13.3	0.322	0.0514	0.0007	0.3760	0.0060	0.8331	323.3	4.2	324.1	4.4
Küplü granitoid	e	537.9	178.3	27.8	0.340	0.0515	0.0007	0.3758	0.0060	0.8531	323.8	4.3	324.0	4.4
Küplü granitoid	g	398.6	132.9	20.6	0.342	0.0514	0.0007	0.3750	0.0056	0.8909	323.1	4.2	323.4	4.1
Küplü granitoid	bc	322.2	117.1	16.8	0.373	0.0515	0.0007	0.3731	0.0063	0.7662	324.0	4.1	321.9	4.7
Küplü granitoid	fc	418.4	187.1	22.4	0.459	0.0517	0.0007	0.3769	0.0053	0.9343	325.2	4.2	324.8	3.9
Küplü granitoid	c	304.4	128.9	16.4	0.434	0.3826	0.0065	0.0523	0.0007	0.7691	328.4	4.2	329.0	4.8
Küplü granitoid	fr	483.7	228.3	25.9	0.484	0.3681	0.0096	0.0513	0.0007	0.5172	322.8	4.2	318.3	7.1
Borçak granitoid	d	104.2	48.0	5.5	0.473	0.3667	0.0078	0.0503	0.0007	0.6402	316.6	4.2	317.2	5.8
Borçak granitoid	e	106.6	45.8	5.5	0.441	0.3545	0.0090	0.0499	0.0007	0.5155	314.2	4.0	308.1	6.7
Borçak granitoid	f	214.4	128.2	11.7	0.613	0.3637	0.0052	0.0508	0.0006	0.8737	319.6	3.9	315.0	3.9
Borçak granitoid	gc	224.1	97.2	12.1	0.445	0.3778	0.0080	0.0525	0.0007	0.6215	329.8	4.2	325.4	5.8
Borçak granitoid	gr	222.3	73.7	11.6	0.340	0.3752	0.0075	0.0518	0.0007	0.6802	325.9	4.3	323.5	5.5
Borçak granitoid	h	269.3	166.5	14.9	0.634	0.3725	0.0063	0.0512	0.0007	0.8168	321.7	4.3	321.5	4.6
Borçak granitoid	i	164.2	108.6	9.2	0.678	0.3794	0.0073	0.0511	0.0007	0.6783	321.0	4.1	326.6	5.3
Borçak granitoid	k	222.6	71.2	11.1	0.328	0.3691	0.0065	0.0500	0.0006	0.7349	314.4	4.0	319.0	4.8
Borçak granitoid	l	234.2	142.5	13.0	0.624	0.3759	0.0069	0.0515	0.0007	0.7130	323.8	4.1	324.0	5.0
Borçak granitoid	m	82.6	32.6	4.3	0.404	0.3648	0.0078	0.0511	0.0007	0.6783	321.1	4.5	315.8	5.8
Borçak granitoid	n	174.2	58.7	8.9	0.346	0.3708	0.0071	0.0507	0.0007	0.7127	318.8	4.2	320.3	5.2
Borçak granitoid	n	134.2	51.4	6.9	0.393	0.3741	0.0083	0.0502	0.0007	0.5881	315.6	4.0	322.7	6.1
Borçak granitoid	o	273.2	93.0	14.1	0.349	0.3726	0.0059	0.0512	0.0007	0.8113	321.6	4.0	321.5	4.3
Borçak granitoid	p	114.0	48.7	5.9	0.439	0.3720	0.0084	0.0498	0.0007	0.6039	313.4	4.2	321.1	6.2

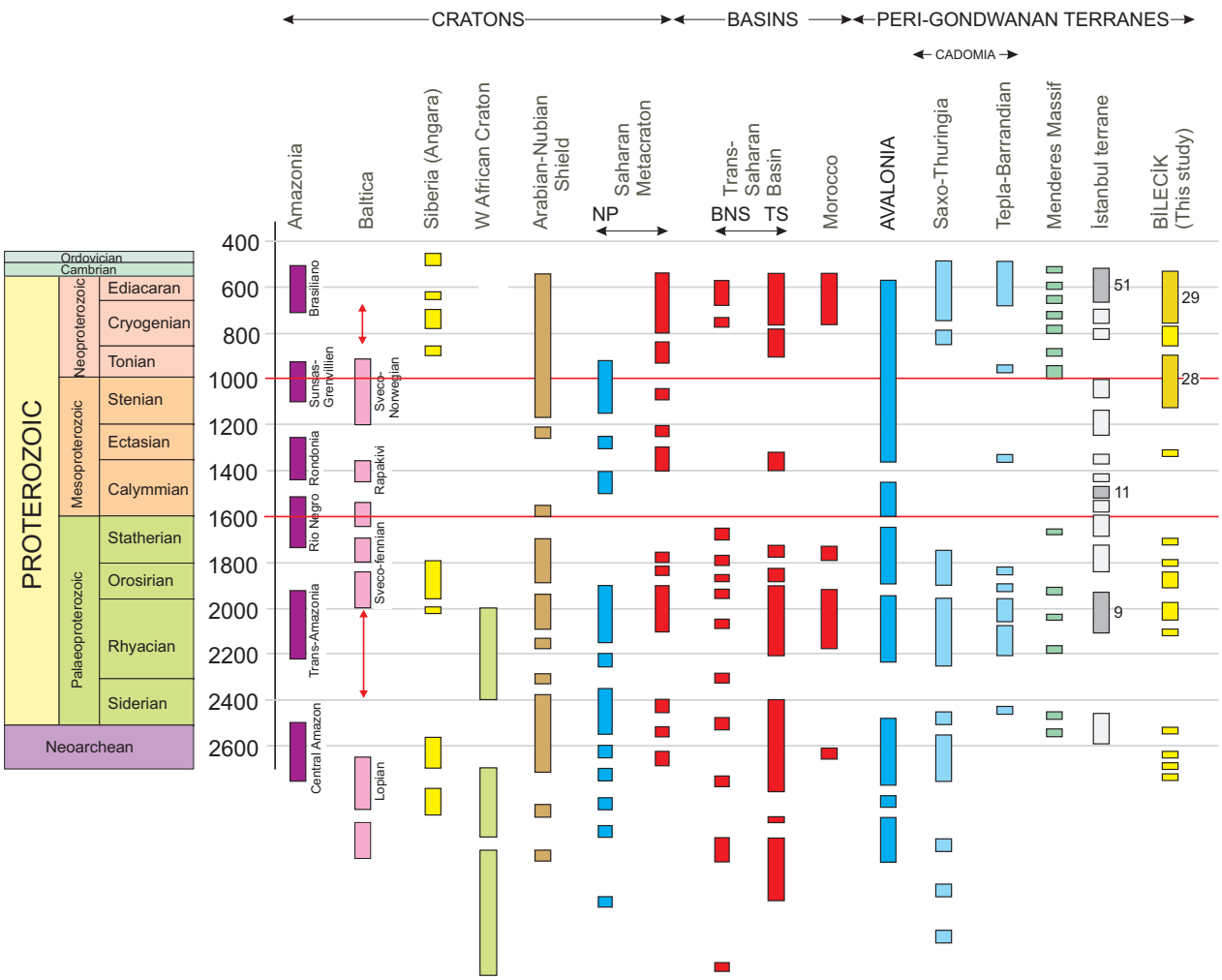

Figure 9. Distribution of detrital zircon ages and/or igneous events known from the major cratons, epi-cratonic basins and peri-Gondwanan terranes. Data sources: Nance & Murphy (1996); Friedl *et al.* (2000, 2004); Strnad & Mihaljevic (2005); Slama *et al.* (2008); Linnemann *et al.* (2004, 2008); Murphy *et al.* (2004a, b, c); Anders *et al.* (2006); Zulauf *et al.* (2007); Sunal *et al.* (2008); P.A. Ustaömer *et al.* (2011); Drost *et al.* (2011) and references therein. The numbers to the right of the bars for the İstanbul terrane and the Central Sakarya basement refer to the number of zircons in the large zircon populations. NP– Neoproterozoic, BNS– Benin-Nigeria Shield, TS– Tuareg Shield.

Nubian Shield, close to the Afro-Arabian margin, are characterised by Grenvillian/Kibaran ages (Zulauf *et al.* 2007). The Arabian-Nubian Shield is interpreted as a collage of arc-type and ophiolitic terranes that were amalgamated during the assembly of eastern Gondwana (Be'eri Shlevin *et al.* 2009 and references therein).

Cambrian–Ordovician sandstones were deposited on the northern periphery of the Arabian-Nubian Shield (e.g., Elat sandstone), as exposed in Jordan and Israel (Avigad *et al.* 2003). Sandstones of this age are also known more locally in the Geyikdağ Unit of the Tauride-Anatolide Platform (i.e. the Seydişehir Formation; Dean & Monod 1970), although no zircon age dating is currently available for these. The zircon populations in the Elat sandstones (Kolodner *et al.* 2006) are notably similar to our results from the Central Sakarya basement (Figure 9), as highlighted by a density probability diagram (Figure 10). The sediments from both our area and the Elat sandstones

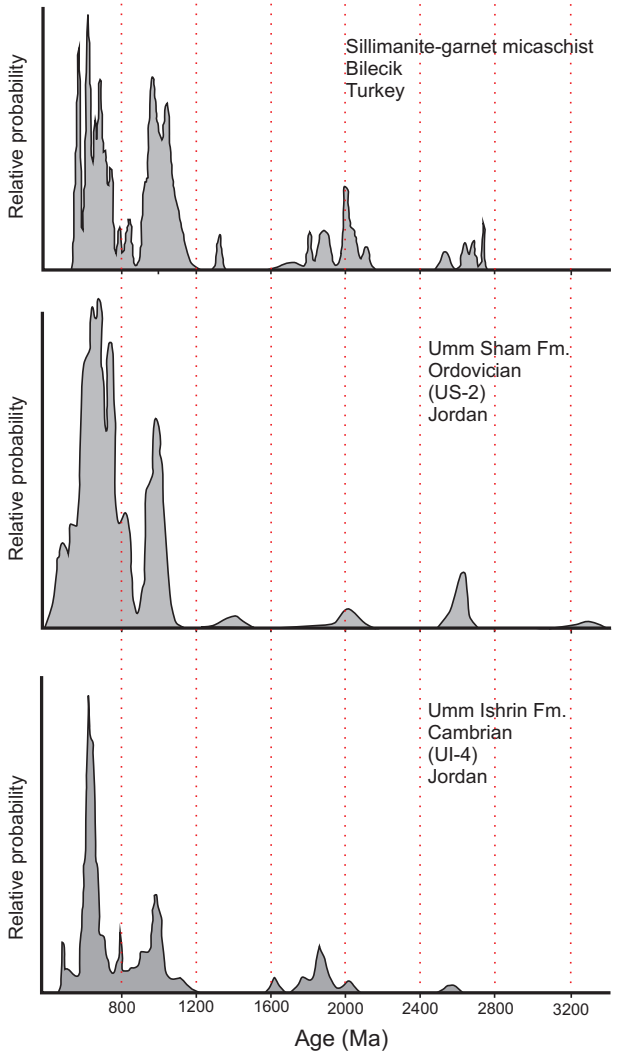

Figure 10. Relative probability histograms of detrital zircon ages from the Central Sakarya basement, compared with those from the Cambrian and Ordovician sedimentary rocks in Jordan (Kolodner *et al.* 2006). Note the similarity of the histograms, with overlapping peaks of similar ages. See also Figure 11.

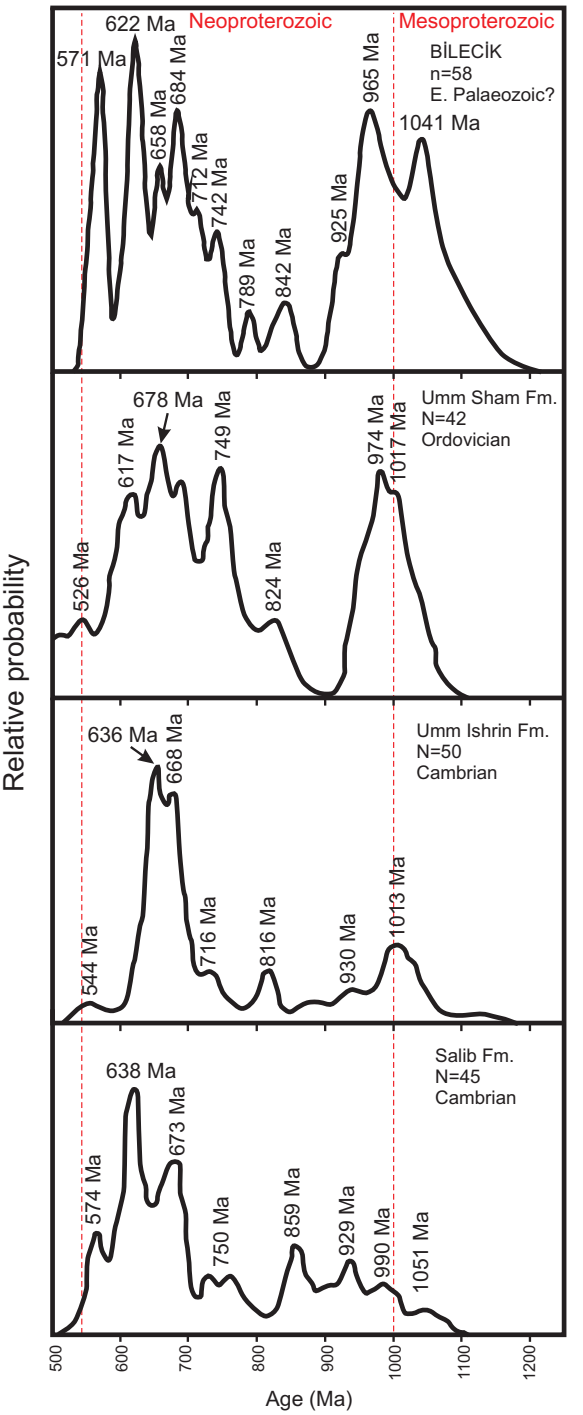

Figure 11. Expanded relative probability histograms of concordant detrital zircon ages < 1.2 Ga from the Central Sakarya basement compared with the Cambrian–Ordovician sediments from Jordan. Note that the peak magmatic periods encountered in both areas are similar and that the Kibaran-aged zircon population is relatively more pronounced in the Central Sakarya basement.

are characterised by the Late Neoproterozoic (0.5–0.75 Ga; 0.8 Ga) and Early Neoproterozoic/late Mesoproterozoic (0.9–1.1 Ga) ages. Both areas are also characterised by similar magmatically quiescent periods. In addition, the two large zircon populations (Figure 11) in both the Central Sakarya and Elat source regions exhibit very similar peak magmatic periods (550 Ma–1.1. Ga). Specifically, peak magmatic periods are dated at 571, 622, 684, 742, 965 and 1041 Ma for the Central Sakarya basement, whereas those

for the Elat sandstone are 574, 638, 678, 750, 974 and 1051 Ma (Kolodner *et al.* 2006).

The Kibaran ages (0.9–1.1 Ga) from the Cambro–Ordovician Elat sandstone have been considered to be enigmatic because of an apparent absence of any suitable nearby source area (Avigad *et al.* 2003; Kolodner *et al.* 2006). A Kibaran-aged zircon population becomes more pronounced upwards in the Elat sandstone succession. Kibaran-aged zircons are very marked in our sample, forming ~35% of the total zircon population. There are two different interpretations about these zircons, either that they are very far travelled or more locally derived. A source area >3000 km to the south of the Levant region has been suggested, either Burundi-Rwanda (Cahen *et al.* 1984; Kolodner *et al.* (2006), or the flanks of Mozambique belt in southeast Africa (Kröner 2001). In this scenario, Neoproterozoic glaciers could have transported large amounts of detritus northwards, followed by fluvial reworking and final deposition as the Cambro–Ordovician Elat sandstone (Avigad *et al.* 2003; Kolodner *et al.* 2006). Alternatively, a much more proximal source of sand existed. For example, suitable protoliths exist in the Negash-Shiraro and Sa'al units of the present-day Sinai Peninsula, which then formed part of the northeastern margin of the northwest Gondwana continent (Be'eri Shlevin *et al.* 2009). Our Kibaran-age zircon grains are mostly well rounded, consistent with either fluvial or aeolian transport (either single or multi-cycle erosion/deposition). Purely glacial transport can be excluded as this would not by itself result in well-rounded zircons. Texture alone cannot distinguish relatively local (up to hundreds of kilometres) from remote (~3000 km) sources. However, a relatively local source (e.g., Taurides/Levant) seems probable.

Timing of Rifting from Source Continent

There are two alternatives for the time of rifting of the Central Sakarya basement terrane, assuming a source area in northeast Gondwana near the Arabian-Nubian shield.

The first involves Early Palaeozoic rifting; i.e. relatively early compared to the 'Minoan terranes' of the Eastern Mediterranean region (e.g., Menderes, Crete, Bitlis) that rifted in Permo–Triassic time. In this case the Central Sakarya basement drifted northwards and accreted to the south-Eurasian margin, resulting in the observed amphibolite facies metamorphism during the Late Palaeozoic Variscan orogeny. The Early Carboniferous granitoids might then have formed in response to slab break-off or delamination. Orogenic collapse or erosion could then have allowed shallow-marine sediments to be deposited on the Central Sakarya basement during Late Carboniferous–Permian time. Similar clastic sediment are inferred to unconformably overlie the paragneiss of the Pulur and Artvin basement units in the Eastern Pontides (A.I. Okay & Şahintürk 1997) from which zircon age populations similar to ours have been reported (T. Ustaömer *et al.* 2010). Northward subduction of Palaeotethys beneath the Sakarya Continent then allowed the Karakaya subduction-accretion complex to be assembled along the southern margin of the Sakarya Continent. The arrival of continental fragments and seamounts resulted in regional deformation and metamorphism during latest Triassic time (Pickett & Robertson 1996; A.I. Okay 2000; Robertson & Ustaömer 2011). This was, in turn, followed by the deposition of Early Jurassic to Upper Cretaceous cover units (Y. Yılmaz *et al.* 1997).

In a second model, rifting from the Arabian-Nubian Shield was delayed until Late Palaeozoic or Early Mesozoic time. In this case, the Early Carboniferous granitoids could represent arc magmatism along the north-Gondwana margin (Göncüoğlu *et al.* 1996; Kibici *et al.* 2010). The Carboniferous amphibolite facies metamorphism could then be attributed to an (unspecified) collisional event. This would have followed by rifting, drifting and accretion to the south-Eurasian margin, either during Permian or Triassic time, prior to or during the assembly of the Karakaya Complex. However, there are several problems with the second model. First, there is no known Permian subduction-accretion complex to the north of the Central Sakarya basement, as implied by this interpretation. Secondly, there is no evidence of comparable Carboniferous Barrovian-type metamorphism in other 'Minoan terranes' in the region (e.g., Bitlis massif; Anatolide-Tauride platform).

In summary, we favour the first tectonic model involving rifting from northeast Gondwana during the Early Palaeozoic, followed by accretion to Eurasia

by Late Palaeozoic time. More data are needed to chart the path of the Sakarya terrane in more detail.

Comparison with Neighbouring Terranes

The adjacent İstanbul terrane in the northwest Pontides (Figures 1 & 2) has been inferred to have a source in the 'Amazonian-Avalonian' region of Gondwana (Kalvoda 2001; Kalvoda *et al.* 2003; Oczlon *et al.* 2007; A.I. Okay *et al.* 2008b; Winchester *et al.* 2006; Bozkurt *et al.* 2008; P.A. Ustaömer *et al.* 2011). This prompts a comparison of our zircon data set from the Sakarya basement.

U-Pb detrital zircon data are available for clastic sedimentary rocks of Early Ordovician and Early Carboniferous (Tournesian–Visean?) ages, representing the lower and uppermost parts of the Palaeozoic stratigraphy of the İstanbul terrane (P.A. Ustaömer *et al.* 2011; N. Okay *et al.* 2011). The Lower Carboniferous turbidites of the İstanbul terrane display two zircon populations; one Late Neoproterozoic and the other Late Devonian–Early Carboniferous. The Central Sakarya basement is unlikely to be the source of the Carboniferous sediments of the İstanbul terrane because 0.9–1.2 Ga-age zircons, the largest zircon population in the Central Sakarya basement, are totally absent from the İstanbul terrane. Thus, two diffent terranes should have existed, one inferred to have an Amazonian-Avalonian source region (İstanbul terrane) and the other a northeast African source region (Sakarya terrane). During Early Carboniferous time, the two terranes were presumably located along different parts of the south Eurasian margin or were separated by unspecified oceanic or continental units. N. Okay *et al.* (2011) infer that the İstanbul terrane was located along the southern margin of Europe to the west of its present position, within central Europe, during Early Carboniferous time. An arc terrane derived from the Armorican source continent is inferred to have collided with the Eurasian margin in this area, resulting in the Early Carboniferous (Tournaisian) turbidites being deposited. The İstanbul terrane subsequently migrated eastwards to the Black Sea area, reaching its present position by the Cretaceous when the Western Black Sea basin rifted. In contrast, the Sakarya terrane and its counterparts further east (Pulur and Artvin units), although also Gondwana derived, accreted further east along the Eurasian margin compared to the position of the İstanbul terrane and subsequently remained in this region.

Conclusions

The age and tectonic history of crystalline basement units in the Sakarya Zone, N Turkey is constrained utilising field, petrographic and ion-probe studies.

Detrital zircons separated from a metasedimentary sillimanite-garnet schist range from 551 Ma (Ediacaran) to 2738 Ma (Neoarchean). The zircon populations cluster at ~550–750 Ma, ~950–1050 Ma and ~2000 Ma, with smaller groupings at ~800 Ma and ~1850 Ma. The presence of a Kibaran (0.9–1.1 Ga) zircon population suggests an affinity with the Arabian-Nubian Shield. The detrital zircon age spectrum of the Cambrian–Ordovician Elat sandstone that was deposited on the northern periphery of the Arabian-Nubian Shield is similar to that of the Sakarya basement.

The Central Sakarya metamorphic basement is cut by a number of granitic intrusions (~ Söğüt magmatics), three of which were dated during this study. An alkali feldspar-rich granite (Küplü granitoid) yielded an age of 324.3±1.5 Ma, while a biotite granite (Çaltı granitoid) was dated at 327.2±1.9 Ma. Another granitic body with biotite and amphibole (Borçak granitoid) yielded a significantly younger age of 319.5±1.1 Ma. Late Early Carboniferous granitic magmatism could, therefore, have been active in the Central Sakarya terrane for up to ~8 Ma. The granitic magmatism is likely to relate to subduction or collision of a Central Sakarya terrane with the Eurasian margin.

The Central Sakarya basement terrane is interpreted as a peri-Gondwanan 'Minoan terrane' that rifted from northeast Africa. Rifting probably took place during the Early Palaeozoic in contrast to other terranes that rifted during the Early Mesozoic. The Central Sakarya terrane accreted to the Eurasian margin during the Early Carboniferous, where it underwent Barrovian-type amphibolite facies metamorphism during the Variscan orogeny. Post-collisional felsic melts intruded the terrane during early Late Carboniferous time. The zircon age population of the Central Sakarya terrane differs from the İstanbul terrane in that 0.9–1.2 Ga-age

zircons are absent. This is consistent with the two terranes being still far apart during Late Palaeozoic time.

Acknowledgements

This work was partly supported by the Yıldız Technical University Research Fund (Project No: 29.13.02.01), the İstanbul University Research Fund (Project No: 5456) and a Royal Society of London grant to the third author to enable the first author to visit Edinburgh University for the ion probe analysis. We thank Richard Hinton for assistance with the Ion Probe dating. Richard Taylor helped with sample preparation. Constructive reviews by Thomas Zack and Osman Candan are acknowledged.

References

Abdüsselamoğlu, M.Ş. 1977. *The Palaeozoic and Mesozoic in the Gebze Region-Explanatory Text and Excursion Guidebook*. 4th Colloquium on the Aegean Region, Excursion 4. İTÜ Maden Fakültesi, İstanbul.

Abramovitz, T., Landes, M., Thybo, H., Jacob, A.W.B. & Prodehl, C. 1999. Crustal velocity structure across the Tornquist and Iapetus Suture Zones – a comparison based on MONA LISA and VARNET data. *Tectonophysics* **314**, 69–82.

Altinli, İ.E. 1973a. Bilecik Jurasiği [The Bilecik Jurassic]. *In*: *Cumhuriyetin 50. Yılı Yerbilimleri Kongresi*, Ankara, 103–122 [in Turkish with English abstract].

Altinli, İ.E. 1973b. Orta Sakarya jeolojisi [Geology of the Central Sakarya]. *In: Cumhuriyetin 50. Yılı Yerbilimleri Kongresi*, Ankara, 159–190 [in Turkish with English abstract].

Anders, B., Reischmann, T., Kostopoulos, D. & Poller, U. 2006. The oldest rocks of Greece: first evidence for a Precambrian terrane within the Pelagonian Zone. *Geological Magazine* **143**, 41–58.

Avigad, D., Kolodner, K., Mcwilliams, M., Persing, H. & Weissbrod, T. 2003. Origin of northern Gondwana Cambrian sandstone revealed by detrital zircon SHRIMP dating. *Geology* **331**, 227–230.

Aysal, N., Ustaömer, T., Öngen, S., Keskin, M., Köksal, F., Peytcheva, I. & Fanning, M. 2012. Origin of the Early–Middle Devonian magmatism in the Sakarya Zone, NW Turkey: geochronology, geochemistry and isotope systematics. *Journal of Asian Earth Sciences* **45**, 201–222.

Bandres, A., Eguíluz, L., Ibarguchi, J.I.G. & Palacios, T. 2002. Geodynamic evolution of a Cadomian arc region: the northern Ossa-Morena zone, Iberian massif. *Tectonophysics* **352**, 105–120.

Be'eri-Shlevin, Y., Katzir, Y., Whitehouse, M.J. & Kleinhanns, I.C. 2009. Contribution of pre Pan-African crust to formation of the Arabian Nubian Shield: new secondary ionization mass spectrometry U-Pb and O studies of zircon. *Geology* **37**, 899–902.

Bozkurt, E., Winchester, J.A., Yiğitbaş¸ E. & Ottley, C.J. 2008. Proterozoic ophiolites and mafic–ultramafic complexes marginal to the İstanbul Block: an exotic terrane of Avalonian affinity in NW Turkey. *Tectonophysics* **461**, 240–251.

Cahen, L., Snelling, N.J., Delhal, H. & Vatt, J.R. 1984. *The Geochronology and Evolution of Africa*. Clarendon Press, Oxford.

Chantraine, J., Egal, E., Thiéblemont, D., Le Goff, E., Guerrot, C., Ball'evre M. & Guennoc, P. 2001. The Cadomian active margin (North Armorican Massif, France): a segment of the north Atlantic Panafrican belt. *Tectonophysics* **331**, 1–18.

Chen, F., Siebel, W., Satir, M., Terzİoğlu, M.N. & Saka, K. 2002. Geochronology of the Karadere Basement (NW Turkey) and implications for the geological evolution of the İstanbul Zone. *International Journal of Earth Sciences* **91**, 469–481.

Compston, W. 2004. SIMS U-Pb zircon ages for the Upper Devonian Snobs Creek and Cerberean Volcanics from Victoria, with age uncertainty based on UO_2/UO vs UO/U precision. *Journal of the Geological Society, London* **161**, 223–228.

Compston, W., Williams, I.S. & Meyer, C. 1984. U-Pb geochronology of zircons from lunar breccia 73217 using a sensitive high-resolution ion microprobe. *Journal of Geophysical Research* **89** *Supplement*, B525–534.

Çoğulu, E., Delaloye, M. & Chessex, R. 1965. Sur l'age de quelques roches plutoniques acides dans la région d'Eskişehir, Turquie. *Archive Science de Genéve* **18**, 692–699.

Çoğulu, H.E. & Krummenacher, D. 1967. Problémes géochronométriques dans le partie NW de l'Anatolie Centrale (Turquie). *Schweizerische Mineralogische und Petrographische Mitteilungen* **47**, 825–831.

Dean, W.T. & Monod, O. 1970. The Lower Paleozoic stratigraphy and faunas of the Taurus Mountains near Beyşehir, Turkey. *I. Stratigraphy: Bulletin of the British Museum (Natural History) Geology* **19**, 411–426.

Demİrkol, C. 1977. Üzümlü-Tuzaklı (Bilecik) dolayının jeolojisi [Geology of the Üzümlü-Tuzaklı (Bilecik Province) area]. *Türkiye Jeoloji Kurumu Bülteni* **20**, 9–16 [in Turkish with English abstract].

Dörr, W., Zulauf, G., Fiala, J., Franke, W. & Vejnar, Z. 2002. Neoproterozoic to Early Cambrian history of an active plate margin in the Teplá Barrandian unit – a correlation of U-Pb Isotopic-Dilution-TIMS ages (Bohemia, Czech Republic). *Tectonophysics* **352**, 65–85.

Drost, K., Gerdes, A., Jeffries, T., Linnemann, U. & Storey, C. 2011. Provenance of Neoproterozoic and early Paleozoic siliciclastic rocks of the Teplá Barrandian unit (Bohemian Massif): evidence from U-Pb detrital zircon ages. *Gondwana Research* **19**, 213–231.

Duru, M., Gedik, İ. & Aksay, A. 2002. *1/100.000 Ölçekli Türkiye Jeoloji Haritaları, Adapazarı H24 Paftası [Geological Map of the Adapazarı H24 Quadrangle, 1:100,000 Scale]*. MTA Genel Müdürlüğü, Jeoloji Etüdleri Dairesi.

Duru, M., Pehlivan, Ş., Dönmez, M., Ilgar, A. & Akçay, A.E. 2007. *1/100.000 Ölçekli Türkiye Jeoloji Haritaları, Bandırma H18 Paftası [Geological Map of the Bandırma-H18 Quadrangle 2007, 1:100,000 Scale]*. MTA Genel Müdürlüğü, Jeoloji Etüdleri Dairesi.

Erdoğan, B., Akay, E., Hasözbek, A., Satir, M. & Siebel, W. 2009. Kazdağ Massif (NW Turkey): metamorphic equivalent of the Mesozoic platform of Sakarya Continent. *Goldschmidt Conference Abstracts*, *A335*, Davos-Switzerland.

Fernández-Suárez, J., Gutiérrez-Alonso, G. & Jeffries, T.E. 2002. The importance of along-margin terrane transport in northern Gondwana: insights from detrital zircon parentage in Neoproterozoic rocks from Iberia and Brittany. *Earth and Planetary Science Letters* **204**, 75–88.

Friedl, G., Finger, F., McNaughton, N.J. & Fletcher, I.R. 2000. Deducing the ancestry of terranes: SHRIMP evidence for South America-derived Gondwana fragments in central Europe. *Geology* **28**, 1035–1038.

Friedl, G., Finger, F., Paquette, J.L., Von Quadt, A., McNaughton, N.J. & Fletcher, I.R. 2004. Pre-Variscan geological events in the Austrian part of the Bohemian Massif deduced from U–Pb zircon ages. *International Journal of Earth Sciences* **93**, 802–823.

Göncüoğlu, M.C., Turhan, N., Şentürk, K., Uysal, Ş., Özcan, A. & Işık, A. 1996. *Nallıhan-Sarıcakaya Arasında Orta Sakarya'daki Yapısal Birimlerin Jeolojik Özellikleri [Geological Characteristics of the Structural Units in Central Sakarya Between Nallıhan-Sarıcakaya]*. MTA Report no. **10094** [in Turkish, unpublished].

Göncüoğlu, M.C., Dirik, K. & Kozlu, H. 1997. General characteristics of pre-Alpine and Alpine terranes in Turkey: explanatory notes to the terrane map of Turkey. *Annales Géologique des Pays Hellénique* **37**, 515–536.

Göncüoğlu, M.C., Turhan, N., Şentürk, K., Özcan, A., Uysal, Ş. & Yalınız, M.K. 2000. A geotraverse across NW Turkey: tectonic units of the Central Sakarya region and their tectonic evolution. *In:* Bozkurt, E., Winchester, J.A. & Piper, J.A.D. (eds), *Tectonics and Magmatism in Turkey and Surrounding Area*. Geological Society, London, Special Publications **173**, 139–161.

Greiling, R.O., Jensen, S. & Smith, A.G. 1999. Vendian–Cambrian subsidence of the passive margin of western Baltica-application data from the Scandinavian Caledonides. *Norsk Geologisk Tidsskrift* **79**, 133–144.

Gubanov, A.P. 2002. Early Cambrian palaeogeography and the probable Iberia-Siberia connection. *Tectonophysics* **352**, 153–168.

Gutiérrez-Alonso, G., Fernández-Suárez, J., Jeffries, T.E., Jenner, G.A., Tubrett, M.N., Cox, R. & Jackson, S.E. 2003. Terrane accretion and dispersal in the northern Gondwana margin. An Early Paleozoic analogue of a long-lived active margin. *Tectonophysics* **365**, 1–12.

Gürsu, S. & Göncüoğlu, M.C. 2005. Early Cambrian back-arc volcanism in the western Taurides, Turkey: implications for the rifting along northern Gondwanan margin. *Geological Magazine* **142**, 617–631.

Guterch, A., Grad, M., Thybo, H. & Keller, G.R. 1999. POLONAISE-97- an international seismic experiment between Precambrian and Variscan Europe in Poland. *Tectonophysics* **314**, 101–121.

Hartz, E.H. & Torsvik, T.H. 2002. Baltica upside down: a new plate tectonic model for Rodinia and the Iapetus Ocean. *Geology* **30**, 255–258.

Ireland, T.R. & Williams, I.S. 2003. Considerations in zircon geochronology by SIMS. *In:* Hanchar, J.M. & Hoskin, P.W.O. (eds), *Zircon*. Reviews in Mineralogy and Geochemistry, 215–242.

Kadioğlu, Y.K., Kayadibi, Ö. & Aydal, D. 1994. Söğüt magmatitlerinin petrografisi ve jeokimyası [The petrography and geochemistry of the Söğüt-Bilecik magmatites]. *Türkiye Jeoloji Kurultayı Bülteni* **9**, 1–10 [in Turkish with English abstract].

Kalvoda, J. 2001. Upper Devonian–Lower Carboniferous foraminiferal paleobiogeography and peri-Gondwana terranes at the Baltica-Gondwana interface. *Geologica Carpathica* **52**, 205–215.

Kalvoda, J., Leichmann, J., Ba´bek, O. & Melichar, R. 2003. Brunovistulian terrane (Central Europe) and İstanbul Zone (NW Turkey): Late Proterozoic and Paleozoic tectonostratigraphic development and paleogeography. *Geologica Carpatica* **54**, 139–152.

Kibici, Y. 1991. Orta Sakarya havzasındaki derinlik kayaçlarının petrografisi ve petrokimyasal özellikleri [Petrography and petrochemical characteristics of the intrusive rocks in the Central Sakarya basin]. *Akdeniz Üniversitesi Isparta Mühendislik Fakültesi Dergisi* **5**, 1–31 [in Turkish with English abstract].

Kibici, Y. 1999. Geochemical properties and genetical interpretation of the central Sakarya region granitoid belt. *Afyon Kocatepe University, Journal of Science* **1**, 143–157.

Kibici, Y., İlbeyli, N., Yildiz, A. & Bağci, M. 2010. Geochemical constraints on the genesis of the Sarıcakaya intrusive rocks, Turkey: Late Paleozoic crustal melting in the central Sakarya Zone. *Chemie der Erde* **70**, 243–256.

Kolodner, K., Avigad, D., McWilliams, M., Wooden, J.L., Weissbrod, T. & Feinstein, S. 2006. Provenance of north Gondwana Cambrian–Ordovician sandstone: U-Pb SHRIMP dating of detrital zircons from Israel and Jordan. *Geological Magazine* **143**, 367–391.

Kröner, A., Willner, A.P., Hegner, E., Jaeckel, P. & Nemchin, A. 2001. Single zircon ages, *PT* evolution and Nd isotopic systematics of high grade gneisses in southern Malawi and their bearing on the evolution of the Mozambique belt in southeastern Africa. *Precambrian Research* **109**, 257–291.

Linnemann, U., McNaughton, N.J., Romer, R.L., Gehmlich, M., Drost, K. & Tonk, C. 2004. West African provenance for Saxo-Thuringia (Bohemian Massif): did Armorica ever leave pre-Pangean Gondwana? U-Pb-SHRIMP zircon evidence and the Nd-isotopic record. *International Journal of Earth Sciences* **93**, 683–705.

Linnemann, U., Pereira, F., Jeffries, T.E., Drost, K. & Gerdes, A. 2008. The Cadomian orogeny and the opening of the Rheic Ocean: the diachrony of geotectonic processes constrained by LA-ICP-MS U-Pb zircon dating (Ossa-Morena and Saxo-Thuringian Zones, Iberian and Bohemian Massifs). *Tectonophysics* **461**, 21–43.

Linnemann, U. & Romer, R.L. 2002. The Cadomian orogeny in Saxo-Thuringia, Germany: geochemical and Nd-Sr-Pb isotopic characterization of marginal basins with constraints to geotectonic setting and provenance. *Tectonophysics* **352**, 33–64.

Ludwig, K.R. 2003. User's manual for Isoplot 3.00 - A geochronological toolkit for Microsoft Excel. *Berkeley Geochronology Centre Special Publication* **4**, p. 71.

Meert, J.G. & Torsvik, T.H. 2003. The making and unmaking of a supercontinent: Rodinia revisited. *Tectonophysics* **375**, 261–288.

Meert, J.G. & van der Voo, R. 1997. The assembly of Gondwana 800–550 Ma. *Journal of Geodynamics* **23**, 223–235.

Miller, B.V., Samson, S.D. & D'Lemos, R.S. Time span of plutonism, fabric development, and cooling in a Neoprotenozoic magmatic arc segment: U–Pb age constraints from syn-tectonic plutons, Channel Islands, U.K. *Tectonophysics* **312**, 79–95.

Murphy, J.B., Eguiliz, L. & Zulauf, G. 2002. Cadomian orogens, peri-Gondwanan correlatives and Laurentia-Baltica connections. *Tectonophysics* **352**, 1–9.

Murphy, J.B., Fernández-Suárez, J. & Jeffries, T.E. 2004c. Lithogeochemical and Sm-Nd and U-Pb data from the Silurian–Lower Devonian Arisaig Group clastic rocks, Avalon terrane, Nova Scotia: A record of terrane accretion in the Appalachian-Caledonide orogen. *Geological Society America Bulletin* **116**, 1183–1201.

Murphy, J.B., Fernández-Suárez, J., Jeffries, T.E. & Strachan, T.A. 2004b. U-Pb (LA-ICP-MS) dating of detrital zircons from Cambrian clastic rocks in Avalonia: erosion of a Neoproterozoic arc along the northern Gondwana margin. *Journal of the Geological Society, London* **161**, 243–254.

Murphy, J.B., Fernández-Suárez, J., Keppie, J.D. & Jeffries, T.E. 2004a. Contiguous rather than discrete Paleozoic histories for the Avalon and Meguma terranes based on detrital zircon data. *Geological Society of America Bulletin* **32**, 585–588.

Nance, R.D. & Murphy, J.B. 1994. Contrasting basement isotopic signatures and the palinspastic restoration of peripheral orogens: example from the Neoproterozoic Avalonian-Cadomian belt. *Geology* **22**, 617–620.

Nance, R.D. & Murphy, J.B. 1996. Basement isotopic signatures and Neoproterozoic paleogeography of Avalonian-Cadomian and related terranes in the circum-North Atlantic. *In*: *Geological Society of America, Special Publication* **304**, 333–346.

Nance, R.D., Murphy, J.B., Strachan, R.A., Keppie, J.D., Gutiérrez-Alonzo, G., Fernández-Suárez, J., Quésada, C., Linnemann, U., D'Lemos, R. & Pisarevsky, S.A. 2008. Neoproterozoic–early Palaeozoic tectonostratigraphy and palaeogeography of the peri-Gondwanan terranes: Amazonian v. West African connections. *In*: Ennih, N. & Liegeois, J.P. (eds), *The Boundaries of the West African Craton*. Geological Society, London, Special Publications **297**, 345–383.

Neubauer, F. 2002. Evolution of late Neoproterozoic to early Palaeozoic tectonic elements in Central and Southeast European Alpine mountain belts: review and synthesis. *Tectonophysics* **352**, 87–103.

Nzegge, O.M., Satir, M., Siebel,W. & Taubald, H. 2006. Geochemical and isotopic constraints on the genesis of the Late Paleozoic Deliktaş and Sivrikaya granites from the Kastamonu granitoid belt (Central Pontides, Turkey). *Neues Jahrbuch für Mineralogie Abhandlungen* **183**, 27–40.

Oczlon, M.S., Seghedi, A. & Carrigan, C.W. 2007. Avalonian and Baltican terranes in the Moesian Platform (Southern Europe, Romania/Bulgaria) in the context of Caledonia terranes west of the Trans-European Suture Zone. *Geological Society of America, Special Publication* **423**, 375–401.

Okay, A.I. 2000. Was the Late Triassic orogeny in Turkey caused by the collision of an oceanic plateau? *In:* Bozkurt, E., Winchester, J.A. & Piper, J.A.D. (eds), *Tectonics and Magmatism in Turkey and Surrounding Area*. Geological Society, London, Special Publications **173**, 25–41.

Okay, A.I. 2011. Tavşanlı Zone: the subducted northen margin of the Anatolide-Tauride Block. *Bulletin of the Mineral Research and Exploration (MTA) of Turkey* **142**, 191–221.

Okay, A.I., Bozkurt, E., Satir, M., Yiğitbaş, E., Crowley, Q.G. & Shang, C.K. 2008b. Defining the southern margin of Avalonia in the Pontides: geochronological data from the Late Proterozoic and Ordovician granitoids from NW Turkey. *Tectonophysics* **461**, 252–264.

Okay, A.I. & Göncüoğlu, M.C. 2004. The Karakaya Complex: a review of data and concepts. *Turkish Journal of Earth Sciences* **13**, 77–95.

Okay, A.I., Monod, O. & Monié, P. 2002. Triassic blueschists and eclogites from northwest Turkey: vestiges of the Paleo-Tethyan subduction. *Lithos* **64**, 155–178.

Okay, A.I., Noble, P.J. & Tekin, U.K. 2011. Devonian radiolarian ribbon cherts from the Karakaya Complex, Northwest Turkey: implications for the Paleo-Tethyan evolution. *Comptes Rendus Palevol* **10**, 1–10.

Okay A.İ & Şahintürk, Ö. 1997. Geology of the Eastern Pontides. *In*: Robinson, A. (ed), *Regional and Petroleum Geology of the Black Sea and Surrounding Regions*. American Association of Petroleum Geologists (AAPG) Memoir **68**, 291–311.

Okay, A.I., Satir, M., Maluski, H., Siyako, M., Monié, P., Metzger, R. & Akyüz, H.S. 1996. Paleo- and Neo-Tethyan events in northwest Turkey: Geological and geochronological constraints. *In*: Yin, A. & Harrison, M. (eds), *Tectonics of Asia*. *Cambridge University Press* 420–441.

Okay, A.I., Satir, M., Tüysüz, O., Akyüz, S. & Chen, F. 2001a. The tectonics of the Strandja Massif; late Variscan and mid-Mesozoic deformation and metamorphism in the northern Aegean. *International Journal of Earth Sciences* **90**, 217–233.

Okay, A.I., Satir, M., Zatin, M., Cavazza, W. & Topuz, G. 2008c. An Oligocene ductile strike-slip shear zone: Uludağ Masif, northwest Turkey – implications for the escape tectonics. *Geological Society of America Bulletin* **120**, 893–911.

Okay, A.I., Şengör, A.M.C. & Görür, N. 1994. Kinematic history of the opening of the Black Sea and its effect on the surrounding regions. *Geological Society America Bulletin* **22**, 267–270.

Okay, A.I. Siyako, M. & Burkan, K.A. 1991. Geology and tectonic evolution of the Biga Peninsula, northwest Turkey. *Bulletin of the Technical University of İstanbul* **44**, 191–255.

Okay, A.I. & Tüysüz, O. 1999. Tethyan sutures of northern Turkey. *In:* Durand, B., Jolivet, L., Hovarth, F. & Séranne, M. (eds), *The Mediterranean Basins: Tertiary Extension within the Alpine Orogen Tethyan Sutures of Northern Turkey*. Geological Society, London, Special Publications **156**, 475–515.

Okay, A.I., Tüysüz, O., Satir, M., Özkan-Altiner, S., Altiner, D., Sherlock, S. & Eren, R.E. 2006. Cretaceous and Triassic subduction-accretion, HP-LT metamorphism and continental growth in the Central Pontides, Turkey. *Geological Society of America Bulletin* **118**, 1247–1269.

Okay, A.I. & Whitney, D.L. 2011. Blueschists, eclogites, ophiolites and suture zones in northwest turkey: a review and a field excursion guide. *Ofioliti* **35**, 131–172.

Okay, N., Zack, T., Okay, A.I. & Barth, M. 2011. Sinistral transport along the Trans-European Suture Zone: detrital zircon-rutile geochronology and sandstone petrography from the Carboniferous flysch of the Pontides. *Geological Magazine* **148**, 380–403.

Özgül, N. 2012. Stratigraphy of the İstanbul region. *Turkish Journal of Earth Sciences* **21**, 817–866.

Pickett, E.A. & Robertson, A.H.F. 1996. Formation of the Late Palaeozoic–Early Mesozoic Karakaya Complex and related ophiolites in NW Turkey by Palaeotethyan subduction-accretion. *Journal of the Geological Society, London* **153**, 995–1009.

Pickett, E.A. & Robertson, A.H.F. 2004. Significance of the volcanogenic Nilüfer Unit and related components of the Triassic Karakaya Complex for Tethyan subduction/accretion processes in NW Turkey. *Turkish Journal of Earth Sciences* **12**, 97–144.

Pin, C., Liñan E., Pascual, E., Donaire, T. & Valenzuela, A. 2002. Late Neoproterozoic crustal growth in the European Variscides: Nd isotope and geochemical evidence from the Sierra de Córdoba Andesites (Ossa-Morena Zone, Southern Spain). *Tectonophysics* **352**, 133–151.

Quésada, C. 1990. Precambrian successions in SW Iberia: their relationship to Cadomian orogenic events. *In*: D'Lemos, R.S., Strachan, R.A. & Topley, C.G. (eds), *The Cadomian Orogeny*. Geological Society, London, Special Publications **51**, 353–362.

Robertson, A.H.F., Parlak, O. & Ustaömer, T. 2009. Melange genesis and ophiolite emplacement related to subduction of the northern margin of the Tauride-Anatolide continent, central and western Turkey. *In*: van Hinsbergen, D.J.J., Edwards, M.A. & Govers, R. (eds), *Geodynamics of Collision and Collapse at the Africa–Arabia–Eurasia Subduction Zone*. Geological Society, London, Special Publications **311**, 9–66.

Robertson, A.H.F. & Ustaömer, T. 2004. Tectonic evolution of the Intra-Pontide suture zone in the Armutlu Peninsula, NW Turkey. *Tectonophysics* **381**, 175–209.

Robertson, A.H.F. & Ustaömer, T. 2011. Role of tectonic-sedimentary melange and Permian–Triassic cover units, central southern Turkey in Tethyan continental margin evolution. *Journal of Asian Earth Sciences* **40**, 98–120.

Robertson, A.H.F. & Ustaömer, T. 2012. Testing alternative tectono-stratigraphic interpretations of the Late Palaeozoic–Early Mesozoic Karakaya Complex in NW Turkey: support for an accretionary origin related to northward subduction of Palaeotethys. *Turkish Journal of Earth Sciences* **21**, 961–1007.

Romano, S.S., Dorr, W & Zulauf, G. 2004. Significant Pb loss of Cadomian zircons due to Alpine subduction of pre-Alpine basement of eastern Crete (Greece). *International Journal of Earth Sciences* **93**, 844–859.

Saner, S. 1978. The depositional associations of upper Cretaceous–Palaecene–Eocene times in central Sakarya and petroleum exploration possibilities. *Proceedings of 4th Petroleum Congress of Turkey*, Ankara, 95–115.

Savov, I., Ryan, J., Haydoutov, I. & Schijf, J. 2001. Late Precambrian Balkan-Carpathian ophiolite–a slice of the Pan-African ocean crust?: geochemical and tectonic insights from the Tcherni Vrah and Deli Jovan massifs, Bulgaria and Serbia. *Journal of Volcanology and Geothermal Research* **110**, 299–318.

Schuhmacher, M., De Chambost, E., McKeegan, K.D., Harrison, T.M. & Migeon, H. 1994. In-situ dating of zircon with the CAMECA ims-1270. *In:* Benninghoven, A., Nihei, Y., Shimizu, R. & Werner, H.W. (eds), *Secondary Ion Mass Spectrometry, SIMS IX* A.Wiley, 919–922.

Şengör, A.M.C. 1984. *The Cimmeride Orogenic System and the Tectonics of Eurasia.* Geological Society of America, Special Paper **195**.

Şengör, A.M.C.& Yilmaz, Y. 1981. Tethyan evolution of Turkey, a plate tectonic approach: *Tectonophysics* **75**, 181–241.

Şentürk, K. & Karaköse, C. 1979. *Orta Sakarya Dolaylarının Temel Jeolojisi [Basic Geology of the Central Sakarya Region]*. Mineral Research and Exploration Institute of Turkey (MTA) Report no. **6642** [in Turkish, unpublished].

Şentürk, K. & Karaköse, C. 1981. Orta Sakarya Bölgesinde Liyas öncesi ofiyolitlerin ve mavişistlerin oluşumu ve yerleşimi [Pre-Liassic formation and emplacement of the ophiolites and blueschists in the Central Sakarya region]. *Türkiye Jeoloji Kurumu Bülteni* **24**, 1–10 [in Turkish with English abstract].

Slama, J., Dunkley, D.J., Kachlik, V. & Kusiak, M.A. 2008. Transition from island-arc to passive setting on the continental margin of Gondwana: U-Pb zircon dating of Neoproterozoic metaconglomerates from the SE margin of the Teplá–Barrandian Unit, Bohemian Massif. *Tectonophysics* **461**, 44–59.

Stern, R.J. 1994. Arc assembly and continental collision in the Neoproterozoic East African Orogen: implications for the consolidation of Gondwanaland. *Annual Review of Earth and Planetary Sciences* **22**, 319–351.

Strnad, L. & Mihaljevič, M. 2005. Sedimentary provenance of Mid-Devonian clastic sediments in the Teplá-Barrandian Unit (Bohemian Massif): U-Pb and Pb-Pb geochronology of detrital zircons by laser ablation ICP-MS. *Mineralogy and Petrology* **84**, 47–68.

Sunal, G., Natal'in, B.A., Satir, M. & Toraman, E. 2006. Paleozoic magmatic events in the Strandja Massif, NW Turkey. *Geodinamica Acta* **19**, 283–300.

Sunal, G., Satir, M., Natal'in, B.A. & Toraman, E. 2008. Paleotectonic position of the Strandja Massif and surrounding continental blocks based on the Pb–Pb age studies. *International Geology Reviews* **50**, 519–545.

Sunal, G., Satir, M., Natal'in, B.A., Topuz, G. & Vonderschmidt, O. 2011. Metamorphism and diachronous cooling in a contractional orogen: the Strandja Massif, NW Turkey. *Geological Magazine* **148**, 580–596.

Teipel, U., Eichhorn, R., Loth, G., Rohrmuller, J., Holl, R. & Kennedy, A. 2004. U–Pb SHRIMP and Nd isotopic data from the western Bohemian Massif (Bayerischer Wald, Germany): implications for Upper Vendian and Lower Ordovician magmatism. *International Journal of Earth Sciences* **93**, 782–801.

Tekeli, O. 1981. Subduction complex of pre-Jurassic age, northern Anatolia, Turkey. *Geology* **9**, 68–72.

Topuz, G., Altherr, R., Satir, M. & Schwarz, W.H. 2004. Low grade metamorphic rocks from the Pulur complex, NE Turkey: implications for pre-Liassic evolution of the Eastern Pontides. *International Journal of Earth Sciences* **93**, 72–91.

Topuz, G., Altherr, R., Schwarz,W.H., Dokuz, A. & Meyer, H.P. 2007. Variscan amphibolite facies metamorphic rocks from the Kurtoğlu metamorphic complex (Gümüşhane area, Eastern Pontides, Turkey). *International Journal of Earth Sciences* **96**, 861–873.

Topuz, G., Altherr, R., Siebel, W., Schwarz , W.H., Zack, T., Hasözbek, A., Barth, M., Satir, M. & Şen, C. 2010. Carboniferous high-potassium I-type granitoid magmatism in the Eastern Pontides: the Gümüşhane pluton (NE Turkey). *Lithos* **116**, 92–110.

Tüysüz, O. 1990. Tectonic evolution of a part of the Tethyside orogenic collage: the Kargı Massif, northern Turkey. *Tectonics* **9**, 141–160.

Unrug, R., Haranczyk, C. & Chocyk-Jaminska, M. 1999. Easternmost Avalonian and Armorican-Caledonian terranes of Central Europe and Caledonian-Variscan evolution of the polydeformed Krakow mobile belt: geological constraints. *Tectonophysics* **302**, 133–157.

Ustaömer, P.A., Mundil, R. & Renne, P. 2005. U/Pb and Pb/Pb zircon ages for arc-related intrusions of the Bolu Massif (W Pontides, NW Turkey): evidence for Late Precambrian (Cadomian) age. *Terra Nova* **17**, 215–223.

Ustaömer, P.A., Ustaömer, T. & Robertson, A.H.F. 2010. Ion Probe U-Pb dating of the Central Sakarya basement: a peri-Gondwana terrane cut by late Lower Carboniferous subduction/collision related granitic magmatism. *Geophysical Research Abstracts* **12**, EGU 2010-5966.

Ustaömer, P.A., Ustaömer, T., Collins, A.S. & Robertson, A.H.F. 2009. Cadomian (Ediacaran–Cambrian) arc magmatism in the Bitlis Massif, SE Turkey: magmatism along the developing northern margin of Gondwana. *Tectonophysics* **475**, 99–112.

Ustaömer, P.A., Ustaömer, T., Gerdes, A. & Zulauf, G. 2011. Detrital zircon ages from Ordovician quartzites of the İstanbul exotic terrane (NW Turkey): evidence for Amazonian affinity. *International Journal of Earth Sciences* **100**, 23–41.

Ustaömer, T. & Robertson, A.H.F. 1993. A Late Palaeozoic–Early Mesozoic marginal basin along the active southern continental margin of Eurasia: evidence from the Central Pontides (Turkey) and adjacent regions. *Geological Journal* **28**, 219–238.

Ustaömer, T. & Robertson, A.H.F. 1997. Tectonic-sedimentary evolution of the North-Tethyan active margin in the Central Pontides of Northern Turkey. *In:* Robinson, A.G. (ed), *Regional and Petroleum Geology of the Black Sea Region*. American Association of Petroleum Geologists (AAPG) Memoir **68**, 245–290.

Ustaömer, T. & Robertson, A.H.F. 2010. Late Palaeozoic–Early Cenozoic tectonic development of the Eastern Pontides (Artvin area), Turkey: stages of closure of Tethys along the southern margin of Eurasia. *In:* Stephenson, R.A., Kaymakci, N., Sosson, M., Starostenko, V. & Bergerat, F. (eds), *Sedimentary Basin Tectonics from the Black Sea and Caucasus to the Arabian Platform*. Geological Society, London, Special Publications **340**, 281–327.

Ustaömer, T. & Robertson, A.H.F., Gerdes, A. & Ustaömer, P.A. 2010. Timing of peak Variscan metamorphism of a NE Gondwana-derived terrane in the Artvin-Yusufeli area, NE Pontides, NE Turkey: evidence from U-Pb LA-ICP-MS dating of paragneiss. *7th International Symposium on Eastern Mediterranean Geology, Abstract Book*, p. 8.

Whitehouse, M.J., Claesson, S., Sunde, T. & Vestin, J. 1997. Ion microprobe U-Pb geochronology and correlation of Archaean gneisses from the Lewisian Complex of Gruinard Bay, northwestern Scotland. *Geochimica Cosmochimica Acta* **61**, 4429–4438.

Wiedenbeck, M., Alle, P., Corfu, F., Griffin, W.L., Meier, M., Oberli, F., Von Quadt, A., Roddick, J.C. & Spiegel, W. 1995. Three natural zircon standards for U-Th-Pb, Lu-Hf, trace element and REE analyses. *Geostandards Newsletter* **19**, 1–23.

Williams, I.S. 1998. U-Th-Pb geochronology by ion microprobe. *In:* McKibben, M.A., Shanks, W.C. & Ridley, W.I. (eds), *Applications of Microanalytical Techniques to Understanding Mineralizing Processes, Socorro, New Mexico*. Reviews in Economic Geology, Society of Economic Geologists **7**, 1–35.

Williams, I.S. & Claesson, S. 1987. Isotopic evidence for the Precambrian provenance and Caledonian metamorphism of high-grade paragneisses from the Seve Nappes, Scandinavian Caledonides: 2. Ion microprobe zircon U-Th-Pb. *Contributions to Mineralogy and Petrology,* **97**, 205–217.

Winchester, J.A., Pharaoh, T.C., Verniers, J., Ioane, D. & Seghedi, A. 2006. Palaeozoic accretion of Gondwana-derived terranes to the East European Craton: recognition of detached terrane fragments dispersed after collision with promontories. *In:* Gee, D.G. & Stephenson, R. (eds), *European Lithosphere Dynamics*. Geological Society, London, Memoirs **32**, 323–332

Yilmaz, O. 1979. *Daday-Devrekani Masifi Kuzeydoğu Kesimi Metamorfik Petrolojisi* [*Metamorphic Petrology of the Northeastern Part of Daday-Devrekani Massif*]. Habilitation Thesis, Hacettepe University [in Turkish with English abstract, unpublished].

Yilmaz, Y. 1977. *Bilecik-Söğüt Dolayındaki Eski Temel Karmaşığı'nın Petrojenetik Evrimi* [*Petrogenetic Evolution of the Old Basement Complex in the Bilecik-Söğüt Area]*. Habilitation Thesis, İstanbul University [in Turkish with English abstract, unpublished].

Yilmaz, Y. 1979. Söğüt-Bilecik bölgesinde polimetamorfizma ve bunların jeotektonik anlamı [Polyphase metamorphism of the Söğüt-Bilecik region and their tectonic implications]. *Türkiye Jeoloji Kurumu Bülteni* **22**, 85–100.

Yilmaz, Y., Tüysüz, O., Yiğitbaş, E., Genç, C.Ş. & Şengör, A.M.C. 1997. Geology and tectonic evolution of the Pontides. *In:* Robinson, A. (ed), *Regional and Petroleum Geology of the Black Sea and Surrounding Regions.* American Association of Petroleum Geologists (AAPG) Memoir **68**, 183–226.

Yilmaz, Y. 1981. Sakarya Kıtası güney kenarının tektonik evrimi [Tectonic evolution of southern margin of the Sakarya Continent]. *İstanbul Yerbilimleri***1**, 33–52.

Zulauf, G., Dörr, W., Fiala, J. & Romano, S.S. 2007. Crete and Minoan terranes: age constraints from U-Pb dating of detrital zircons. *Geological Society of America, Special Publication* **423**, 401–409.